GP60/EE60

Handout #5

From "Earth" by Press + Siever

CHAPTER 18

SEISMOLOGY AND THE EARTH'S INTERIOR

The basic causes of earthquakes are strains induced by plate motions. By their locations and the nature of the ruptures they produce, earthquakes define the plate boundaries. Analysis of seismic waves, together with laboratory studies of rocks, help us to infer the composition and state of the Earth's interior.

Seismology is the study of earthquakes and seismic waves. Because earthquakes are among the scourges of humankind, seismologists are concerned with minimizing their destructiveness. They do this by assessing seismic risks in different geographic regions, so that sensible building and zoning codes can be written, and by researching the problems of tsunamis, earthquake prediction, and even earthquake control. But reducing the hazards of earthquakes is not the only job of seismologists.

By studying the pattern of earthquakes, seismologists have provided one of the essential clues to the development of the concept of plate tectonics: Earthquake belts outline plate boundaries, the zones along which plates collide, diverge, or slide past one another. The modern seismograph, which records the waves generated by earthquakes and explosions, is the most important means of probing the deep interior.

Seismographs

The seismograph is to the Earth scientist what the telescope is to the astronomer—a tool for peering into inaccessible regions. The ideal seismograph would be a "skyhook," a device fixed to a frame outside of the Earth, so that when the ground shakes, the seismic vibrations could be measured by the changing distance between the fixed device and the ground. Because this fixed base is impossible to achieve, a compromise is struck by coupling a mass so loosely to the Earth that the ground can vibrate without causing much motion of the mass. The mass is coupled to the Earth by means of a pendulum (Figure 18-1) or by suspending it from a spring (Figure 18-2). When the ground moves, the mass tends to remain stationary because of its inertia, and the displacement of the Earth relative to the stationary mass is used to sense ground movement. The most advanced electronic technolo-

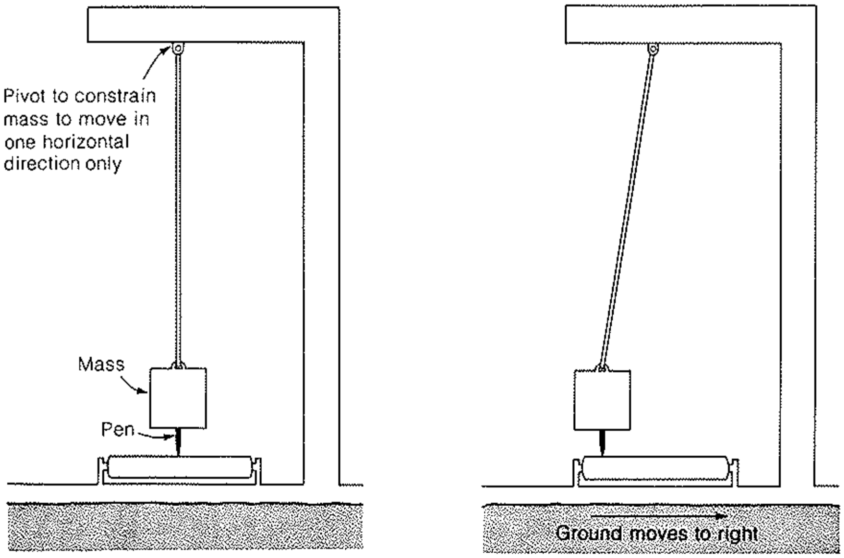

Figure 18-1
The principle of the pendulum-mounted seismograph. Because of its inertia, the mass does not keep up with the motion of the ground. The pen traces the difference in motion between the mass and the ground, in this way recording vibrations that accompany seismic waves. The instrument schematized here records horizontal motion.

gy* is used to magnify this motion, so that modern instruments can detect ground displacements as small as 10^{-8} cm—an astounding feat, considering that such small displacements are of atomic size. This is far more sensitivity than can actually be used on Earth because the ground moves in a continual state of unrest, shaken by the action of the winds, ocean waves, and machinery. In most places such sensitive seismographs would be driven off scale by Earth's "noise." The Moon is the place for this most advanced seismograph; there, no winds, no ocean sounds, no mechanical vibrations can overload it. The lunar seismographs left behind by the astronauts can detect the seismic waves generated by a 1-kilogram (2.2-pound) meteor striking anywhere on the Moon's surface. A well-known seismograph is shown in Figure 18-3.

The strain seismograph shown schematically in Figure 18-4 was developed by H. Benioff, a leader in the design of electronic musical instruments and seismographs. By electronic measurement of the change in distance between two concrete piers about 30 m (100 ft) apart, this instrument can detect stretching and compression of the ground caused by seismic vibrations or by the pull of the Moon on the solid Earth (body tides, just like those to which the ocean responds but much smaller). A record made by a strain seismograph is shown in Figure 18-5, and an actual installation is shown in Figure 18-6.

*For the electronics hobbyist, we might mention that the magnification of a seismograph is achieved by means of moving-coil and variable-reluctance transducers, like those on phonograph pickups, and low-noise, ultra-high-gain, solid-state amplifiers. The output is recorded photogalvanometrically on film, on paper with direct-recording pen motors, on AM or FM or digital magnetic tape. Some unattended seismographs are linked by satellite communication links to central observatories.

Earthquakes

WHAT IS AN EARTHQUAKE?

The rupture of the San Andreas fault that devastated San Francisco in 1906 also provided the

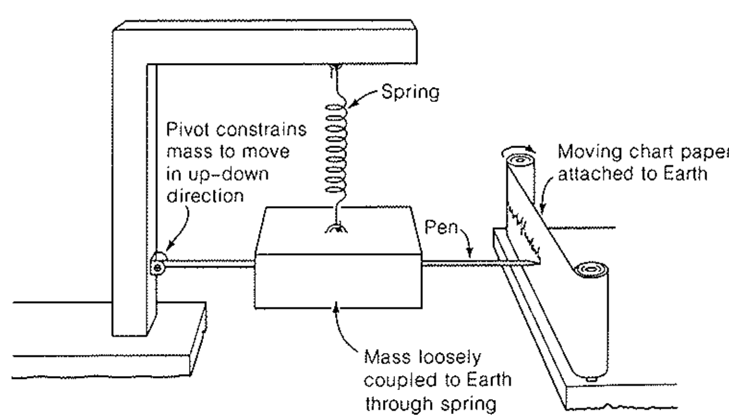

Figure 18-2
Spring-mounted seismograph to record vertical ground motion.

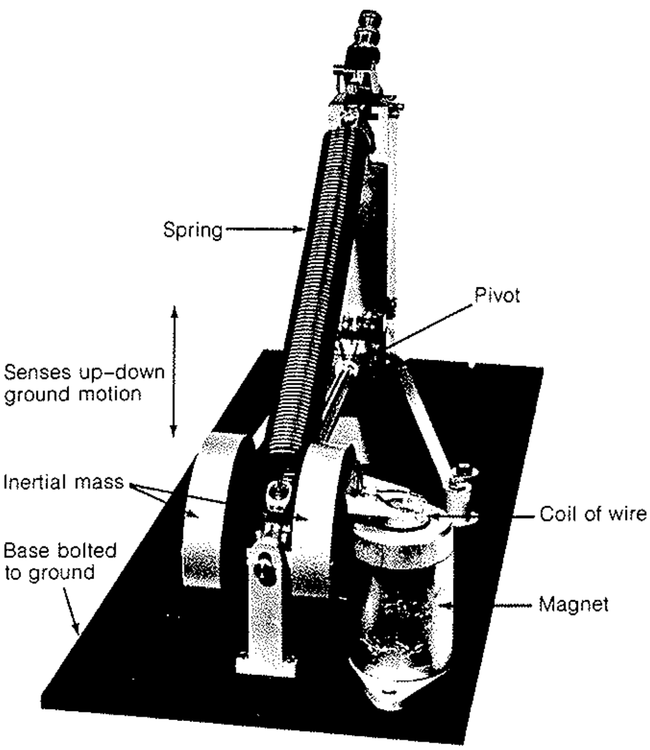

Figure 18-3

The Press-Ewing seismograph, an example of a modern instrument. Airtight cover, electronics, and recording system not shown.

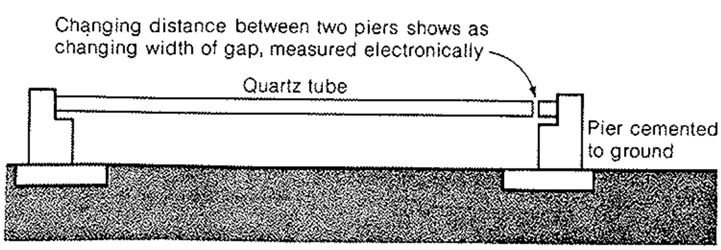

Figure 18-4

The Benioff strain seismograph. The distance between two piers attached to the ground changes as a result of tides in the solid Earth and the passage of seismic waves. These variations are measured by placing an electronic motion detector in the gap.

evidence that led H. F. Reid, one of the official investigators of that catastrophe, to advance his **elastic rebound theory** of earthquakes. Earthquakes are associated with large fractures, or faults, in the Earth's crust and upper mantle. Consider the fault between the two hypothetical crustal blocks in Figure 18-7. Suppose that surveyors had located lines running perpendicular to the fault from block L to block R, are shown in part (a) of the diagram. Blocks L and R are moving in opposite directions, but because they are pressed together by the weight of the overlying rock, friction locks them together, just as a brake can lock the wheel of a car if enough force is applied. Instead of slipping along the fault, the blocks are deformed near the fault, and the surveyors' lines are bent as shown in Figure 18-7b. As the rock is strained, elastic energy is stored in it in the same way that it is stored in a wound-up watch spring. The movement continues, the strain builds up until the frictional bond that locks the fault can no longer hold at some point on the fault, and it breaks (Figures 18-7c, 18-7d, and 18-8). The blocks suddenly slip at this point, which is the **focus** of the earthquake (Figure 18-9). Once the rupture begins, it travels at a speed of about 3.5 km/s (7200 miles/hour), continuing for as much as 1000 km. In great earthquakes, the **slip,** or offset, of the two blocks can be as large as 15 m (50 ft). Figure 18-7d shows the two blocks after the earthquake, displaced by the amount of slip. Once the frictional bond is broken, the elastic strain energy, which has been slowly stored over tens or hundreds of years, is suddenly released in the form of intense seismic vibrations, which constitute the earthquake. The vibrational waves are propagated large distances in all directions from the fault. Near the focus the waves can have large, destructive amplitudes. The process can be likened to storing elastic energy by slowly drawing out the rubber band of a sling shot and then releasing it suddenly to propel a pebble.

Strictly speaking, the elastic rebound theory is an incomplete one. The reason for this is that the pressure holding the blocks together is so great that the frictional bond is actually stronger than the rock itself. In other words, the block should more easily break elsewhere than slip along the fault. Yet faults do exist, and movement occurs along them periodically. To complete the theory, we need a means of "lubricating" the fault or reducing the locking pressure. Geologists working in rock mechanics are currently trying to remove some of the mystery of the mechanics of faulting.

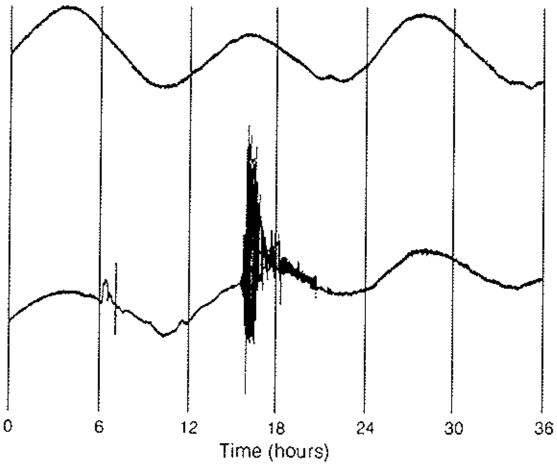

Figure 18-5

Record made by a strain seismograph. The slow periodic movements are the Earth tides; the more rapid vibrations are the seismic waves from an earthquake. [From "Resonant Vibrations of the Earth" by F. Press. Copyright © 1965 by Scientific American, Inc. All rights reserved.]

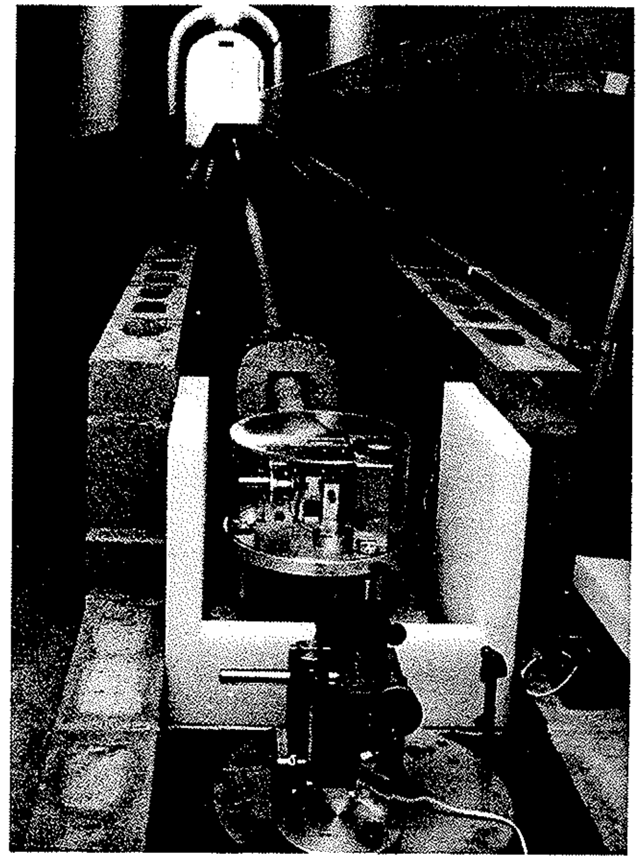

Figure 18-6

A strain seismograph installation in an underground tunnel. This system is so sensitive that it could detect a change of 1 mm in the distance between New York and California.

EARTHQUAKES—HOW BIG AND HOW MANY?

The time between great earthquakes is about 50–100 years in California and somewhat less in more active seismic regions, such as Japan or the Aleutians. Thus the time required to build up the elastic strain energy in the rocks along a fault is enormous compared with the time that elapses during the release of stored energy, for earthquakes last only a few minutes. The amount of stored energy can be gauged in several ways. The two most common methods are to measure the distortion of surveyed lines, as in the example just discussed, or to measure the energy of the released seismic waves. About 10^9 ergs of elastic strain

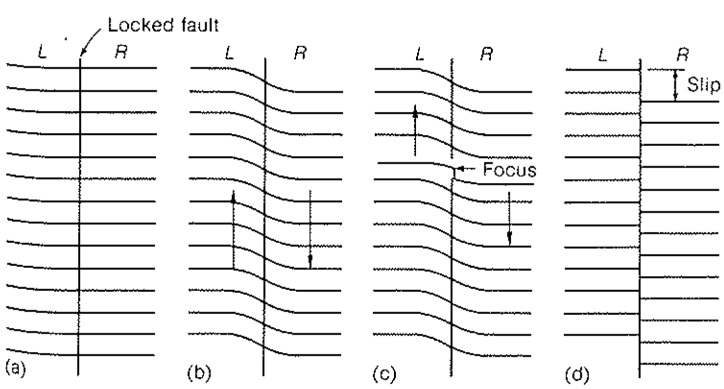

Figure 18-7

The elastic rebound theory of an earthquake. The two simulated crustal blocks L and R are being forced to slide past each other (a). Friction along the fault prevents slip (b), but the deformation builds up until the "frictional lock" is broken (c) and an earthquake slip occurs (d).

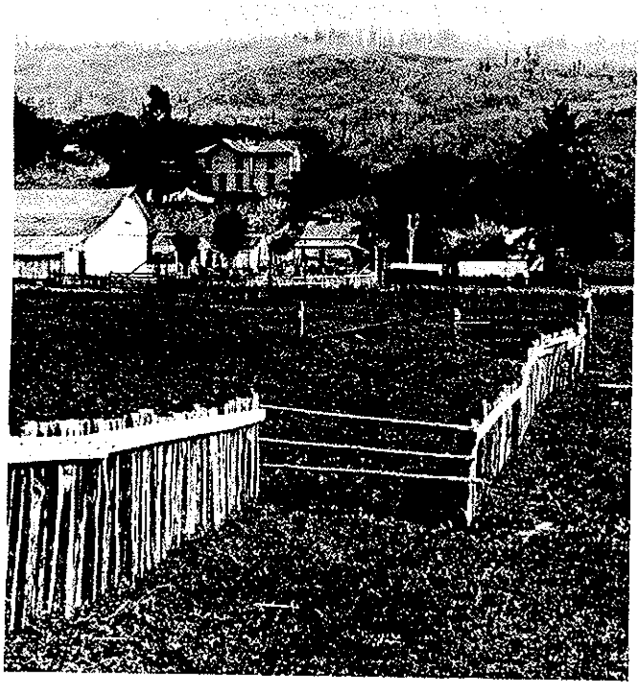

Figure 18-8
The earthquake of 1906 was caused by slip along the San Andreas fault. The offset fence shown here shows a slip of nearly 3 m. The scene is near Bolinas, California. [Photo by G. K. Gilbert; courtesy of R. E. Wallace, U.S. Geological Survey.]

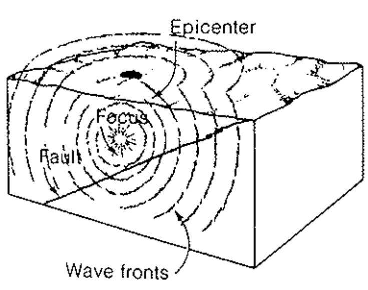

Figure 18-9
The focus of an earthquake is the site of initial slip on the fault. The epicenter is the point on the surface above the focus. Seismic waves radiate from the focus.

energy is released from each cubic meter (1.3 cubic yards) of rock at the time of an earthquake—the equivalent of a fire cracker per cubic meter. This may seem unimpressive until one adds up the cubic meters affected by a great earthquake. Suppose the fault is 1000 km (600 miles) long, extends 100 km downward, and distorts surveyed lines as far as 50 km on either side of the fault. This amounts to a strained volume of 10^{16} m^3, each cubic meter contributing 10^9 ergs, which gives a total of 10^{25} ergs. This is one big fire cracker indeed—about the equivalent of 10,000 nuclear explosions of the strength of the bomb exploded at Hiroshima.

Energy release gives the most precise measure of the size of an earthquake, but it is a long, complicated process to determine the fault dimensions, the slip, and the other factors needed to compute the total energy involved. Seismologists have therefore adopted the **Richter magnitude scale,** which is based on the amplitude of seismic waves recorded by seismographs. Actually, magnitude (m) is based on the logarithm of the maximum amplitude adjusted by a factor that takes into account the weakening of seismic waves as they spread away from the focus. Thus seismologists all over the world can study their records and in a few minutes come up with nearly the same value for the magnitude of an earthquake. Seismographs are sensitive enough to detect earthquakes of magnitude less than 1 quite easily. The largest earthquakes yet recorded have Richter magnitudes of about 8.5. Because these magnitudes are based on a logarithmic scale, an increase in magnitude of one unit corresponds to a tenfold increase in the size of an earthquake as measured by the amplitude of seismic waves. An earthquake of magnitude 8 would be 10,000 ($10^8/10^4$) times one of magnitude 4. Figure 18-10 shows how the magnitude of an earthquake is determined in practice.

Table 18-1 relates magnitude and energy to earthquake effects and indicates the number of earthquakes of given magnitudes each year. The table demonstrates the fortunate fact that most earthquakes are small. Each year, 800,000 little tremors are recorded by instruments but not felt by humans. Great earthquakes, those with magnitudes exceeding 8, occur about once every 5–10 years. Damage begins at magnitude 5 and increases to nearly total destruction in nearby settlements for earthquakes with $m > 8$ ($>$ means "greater than"). The San Fernando (Los Angeles) earthquake of 1971 was only of magnitude 6.6, yet the damage bill amounted to a billion dollars. As damaging as the earthquake was, the seismic

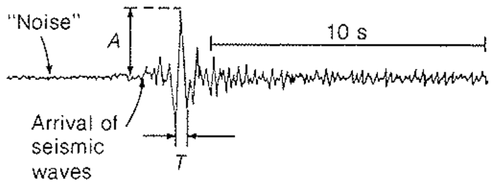

Figure 18-10

Determination of earthquake magnitude from a seismograph recording. Dividing A, the maximum trace motion, by the magnification of the seismograph gives the maximum ground motion a, measured in micrometers (μm; 1 μm = 10^{-4} cm). T is the duration of one oscillation, or the period of the seismic wave in seconds. Magnitude $m = \log(a/T) + B$, where B is a factor that allows for the weakening of seismic waves with increasing distance from the earthquake. *Example:* An earthquake 10,000 km away ($B = 6.8$ from the table of data) produced a ground motion a = 10 μm with period T = 1 s. Thus $m = \log 10 + 6.8 = 7.8$. The correction factor B is found empirically, so that a seismograph located anyplace in the world would give the proper magnitude of an earthquake, regardless of distance to it.

energy release was only about one-thousandth that of some truly great earthquakes, such as those in San Francisco (1906), Toyko (1923), Chile (1960), Alaska (1964), and China (1976). It is no wonder that Californians worry about the great shock that should visit them about every 50–100 years!

Table 18-1 also points up the interesting fact that the few large earthquakes each year release more seismic energy than the hundreds of thousands of small shocks combined. This should put to rest the notion that small earthquakes act as a safety valve, gradually releasing strain in harmlessly small amounts and thus forestalling a big shock. About 10^{26} ergs of seismic energy are released each year. This is about 1% of the heat energy reaching the Earth's surface from the interior, and about 3% of the energy used by humankind..

EARTHQUAKES—WHERE DO THEY OCCUR?

A **seismicity** chart showing the map locations, or **epicenters,** of almost 30,000 earthquakes that occurred between 1961 and 1967 is reproduced in Figure 18-11. A chart compiled in this decade would show the same features. Seismologists have known for decades that earthquakes tend to occur

Table 18-1

Earthquake Magnitudes, Energies, Effects, and Statistics

Characteristic effects of shallow shocks in populated areas	Approximate magnitude	Number of earthquakes per year	Energy (ergs)
Damage nearly total	≥8.0	0.1–0.2	$>10^{25}$
Great damage	≥7.4	4	$\geq 0.4 \times 10^{24}$
Serious damage, rails bent	7.0–7.3	15	$0.04–0.2 \times 10^{24}$
Considerable damage to buildings	6.2–6.9	100	$0.5–23 \times 10^{21}$
Slight damage to buildings	5.5–6.1	500	$1–27 \times 10^{19}$
Felt by all	4.9–5.4	1400	$3.6–57 \times 10^{17}$
Felt by many	4.3–4.8	4800	$1.3–27 \times 10^{16}$
Felt by some	3.5–4.2	30,000	$1.6–76 \times 10^{15}$
Not felt but recorded	2.0–3.4	800,000	$4 \times 10^{10}–9 \times 10^{13}$

Source: Data from B. Gutenberg.

in belts—for example, the "ring of fire" surrounding the Pacific Ocean. In recent years, however, it has become possible to detect the more numerous, smaller earthquakes and to improve methods of locating epicenters, so that seismic belts can now be defined more accurately. Interestingly, the increase in the number of seismic observatories and the use of computers to store and analyze seismic data that made this possible were stimulated by research done in the 1960s, during negoations for a nuclear test-ban treaty; the purpose was to determine whether small underground nuclear explosions could be detected and distinguished seismically from earthquakes.

The new high-quality seismicity maps showed that narrow belts of epicenters coincide almost exactly with the crest of the mid-Atlantic,the east Pacific, and other oceanic ridges, where plates separate. (Compare Figure 18-11 with the map inside the back cover.) Earthquake epicenters are also aligned along transform faults, where plates slide past each other. But earthquakes that originate at depths greater than about 100 km (60 miles) typically occur near margins where plates collide (Figure 18-12). The foci of these earthquakes are distributed on well-defined planes that dip into the mantle, and these occur in close association with deep-sea trenches, island arcs, young mountains, and volcanoes. It is a basic tenet of the theory of plate tectonics that these deep earthquakes actually define the positions of subducted plates, which are plunging back into the mantle beneath an overriding plate (Figure 18-13). This global correlation between topography, geology, and seismicity provided essential data for defining the boundaries of the lithospheric plates. It may seem like a simple matter now to draw a line through the seismic belts and so define the plates depicted on the inside of the back cover, but this important advance could not have been made without the "knowledge explosion" in seismic data and the imaginative, uninhibited, and synthesizing minds of about ten workers who sifted through those data in the years following 1967.

Although most earthquakes are recorded at plate boundaries, the seismicity map shows that a small percentage originate within plates. Some of these have been quite destructive, as is indicated by these examples: New Madrid, Missouri (1812), Charleston, South Carolina (1886), Boston, Massachusetts (1755), T'ang-shan, China (1976). Apparently, stresses within the lithospheric plates occa-

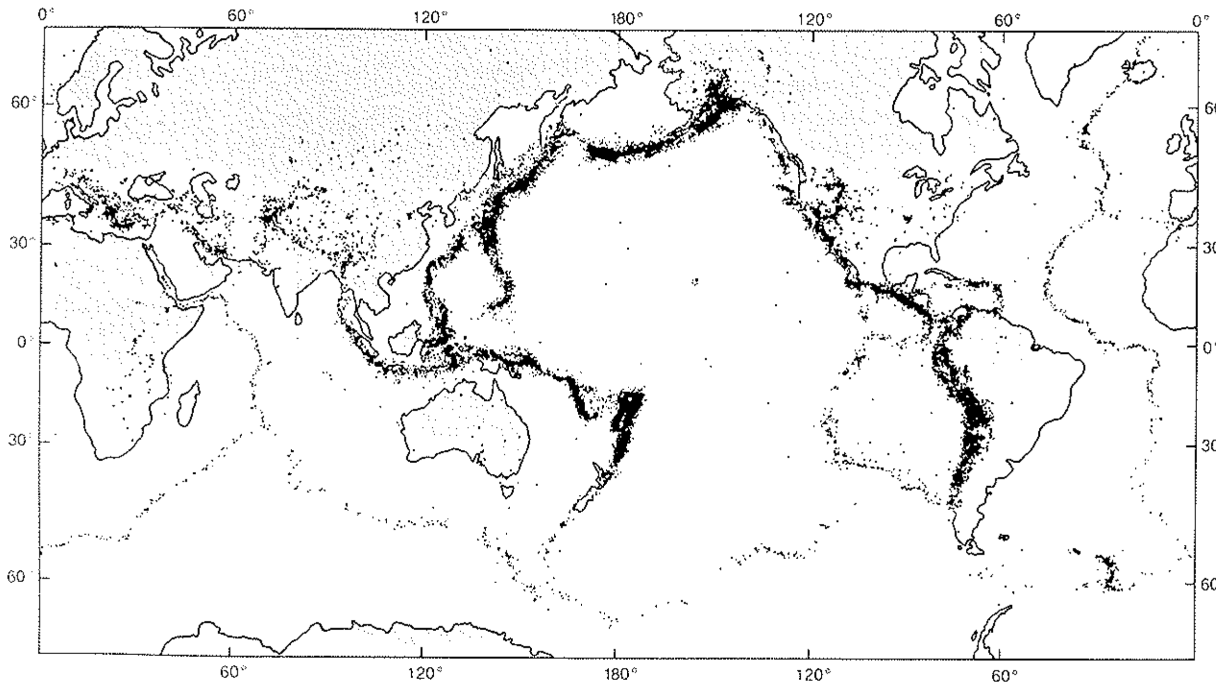

Figure 18-11

Epicenters of some 30,000 earthquakes recorded in the years 1961–1967, with focal depths between 0 and 700 km. [Epicenters by the U.S. Coast and Geodetic Survey. Computer plot by M. Barazangi and J. Dorman, Columbia University.]

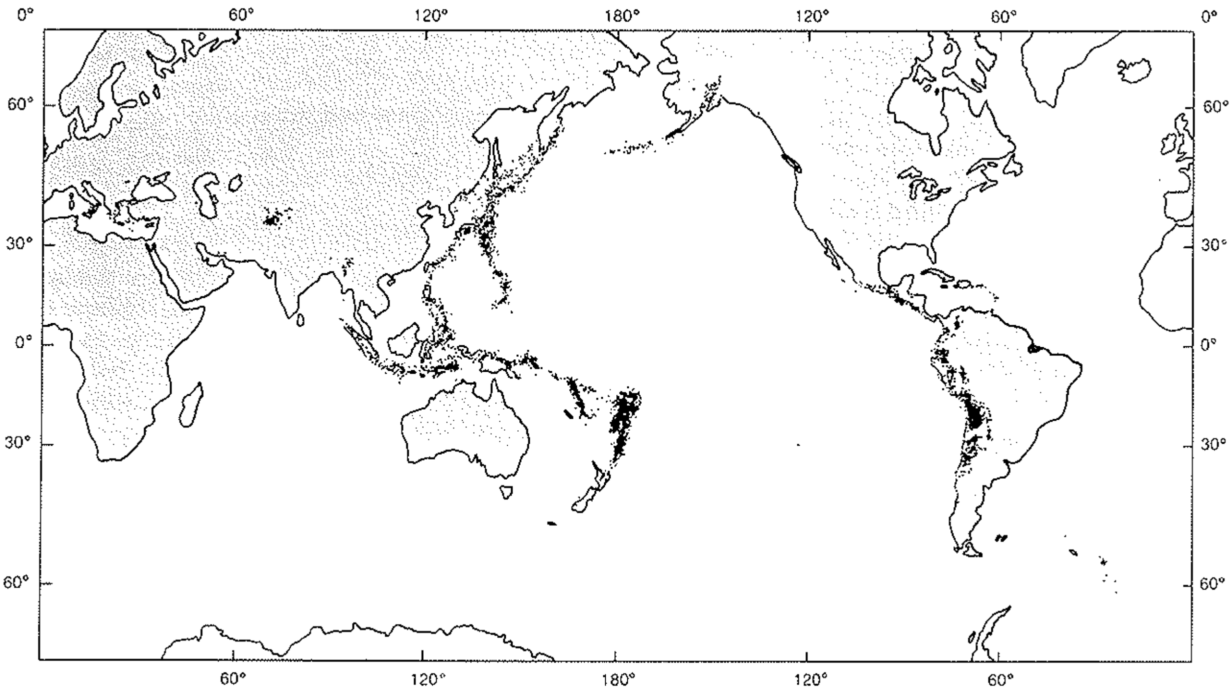

Figure 18-12
Subset of earthquakes from preceding figure with focal depths greater than 100 km. These deep earthquakes typically originate near margins where plates collide and thus serve to identify such plates. [Computer plot by M. Barazangi and J. Dorman, Columbia University.]

sionally build up until they exceed the rock's strength, producing one of these infrequent intraplate earthquakes.

LOCATING THE EPICENTER

The principle involved in identifying a quake's epicenter is quite similar to deducing the distance to a lightning bolt from the time interval between the flash and the sound. Later in this chapter we will describe the two types of seismic waves that travel through the body of the Earth—the first-arriving *P* and the slower-traveling *S* waves, which take almost twice as long to reach the seismograph. Surface waves, a third type, skirt along the surface. The lightning flash may be

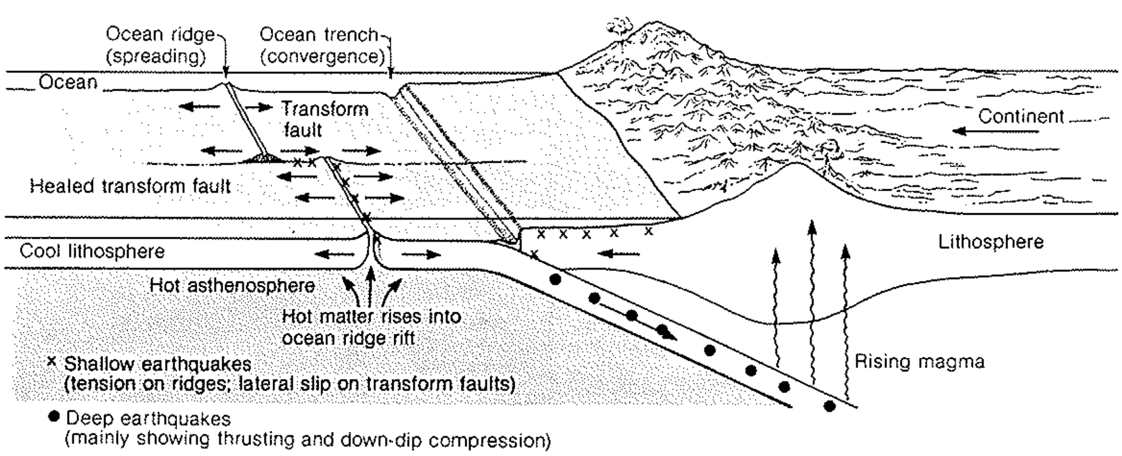

Figure 18-13
The association of earthquakes with three types of plate boundaries: ocean ridges, transform faults, and trenches.

likened to the *P* waves of earthquakes and the thunder to the *S* waves. The time interval between the arrival of *P* and *S* waves therefore increases with the distance traveled by the waves, and with each *S–P* time interval there is associated a definite distance to the epicenter. This is indicated on the travel-time chart for *P* and *S* waves in Figure 18-14, which shows diagrammatically how the travel times of *P* and *S* waves depend on distance and how the *S–P* interval increases with distance. To get an approximation of the epicenter, the seismologists simply read off the *S–P* interval on the seismogram from a given station and use a graph like that in Figure 18-14 or a table to get the distance to the epicenter. Knowing the distances from three or more stations enables them to pinpoint the epicenter (Figure 18-15). They can also deduce the time of the shock at the epicenter because the arrival time of the *P* waves at each station is known, and from a graph or a table it is possible to read about how long the waves took to reach the station. Once an approximation has been made, the exact location can be found by making refinements.

OBTAINING STRESS PATTERNS

When an earthquake occurs, one block slips relative to an adjacent one along a **fault plane** (Figure 18-16a). The orientation of the fault plane and the slip direction are of great interest because they provide information about what is happening at plate boundaries.

If the concept of plate tectonics is correct and seismicity is primarily associated with boundaries along which plates separate, collide, or slide past each other, then the fault orientations and slip directions should differ for each type of plate junc-

Figure 18-14

The time required for *P*, *S*, and surface waves to travel a given distance can be represented by curves on a graph of travel time against distance over the surface. To locate an earthquake epicenter, the time interval observed at a given station is matched against the travel-time curves for *P* and *S* waves until the distance is found at which the separation between the curves agrees with the observed *S−P* time difference. Knowing the distance from the three stations *A*, *B*, and *C*, we can locate the epicenter as in Figure 18-15.

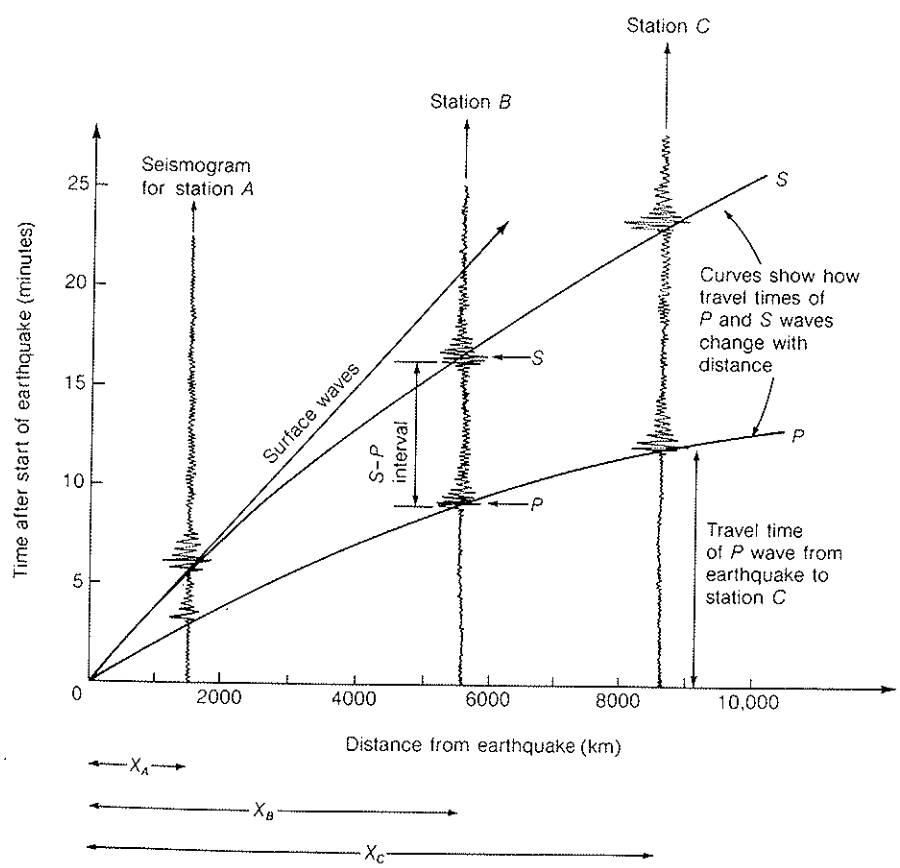

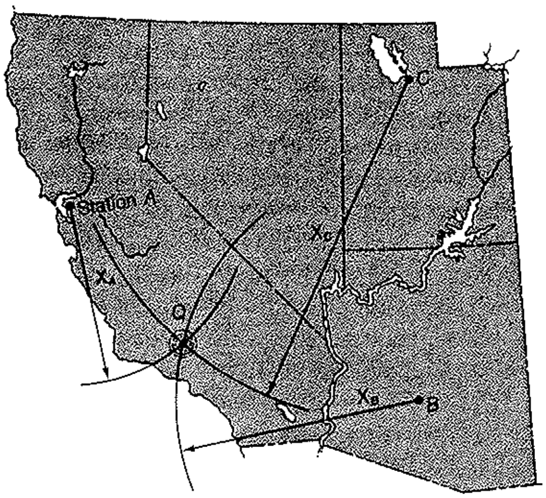

Figure 18-15

Knowing the distance, say X_A, of an earthquake from a given station, as by the method of the preceding figure, we can say only that the earthquake lies on a circle of radius A, centered on the station. If, however, we know the distances from two additional stations B and C, we can infer that the three circles centered on the three stations, with radii X_A, X_B, X_C, intersect uniquely at the point Q, the epicenter.

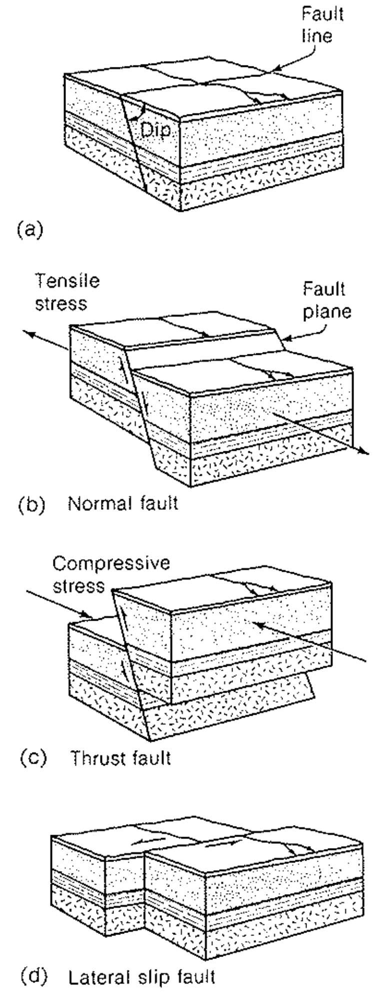

Figure 18-16

The types of fault movement and the stresses that cause them: (a) situation before movement takes place; (b) normal fault due to tensile stress; (c) thrust (or reverse) fault due to compressive stress; (d) lateral slip (or strike slip) fault due to shearing stress.

tion. Earthquakes in divergence zones should result from tension, as if the plates were being pulled apart, and **normal faults,** in which the overlying block moves down the dip of the fault plane, should characterize the earthquake mechanism (Figure 18-16b). Many earthquakes in convergence zones, where plates collide, should show a compressive mechanism—for example, **thrust faulting,** in which the overlying block moves up the dip of the fault plane (Figure 18-16c). Where plates slide past each other along transform faults, the earthquake mechanism should be simple lateral (sideways) slip along nearly vertical planes (Figure 18-16d).

Seismologists have learned to deduce which of these earthquake mechanisms is involved from seismograms. This ability is especially convenient, since very few earthquake faults break through to the surface, where the slip direction and fault orientation can be observed directly, and many small faults are not always so clearly and unambiguously displayed in the field as they are in our illustrations. Seismographs located in different directions from an earthquake epicenter characteristically record seismic waves with an initial motion of the ground either toward the epicenter or away from it, as shown in Figure 18-17. This "radiation pattern" is shown in idealized form as a distribution of outward and inward motions into four quadrants defined by an extension of the fault plane. From such a distribution seismologists can deduce the orientation of the fault plane and the direction of slip, as indicated in the figure.*

*Actually, a fault perpendicular to the one shown in the figure would produce the same pattern of up and down motions if the slip directions were $\leftrightarrows$ rather than $\updownarrows$. Fortunately, however, the correct orientation of the fault plane can be deduced either from field evidence, if there is any, or from the aftershocks that follow the main event, for they originate in the fault plane, and their positions define the true orientation of the fault.

Although Figure 18-17 simplifies nature somewhat and real seismograph stations are not situated in simple circles around faults, seismologists know how to allow for natural complexities and can uncover the true source mechanism of an earthquake from the radiation pattern of P waves. What they find is the following: When the topography of mid-ocean ridges is examined in detail, the ridges are often found to be segmented, the segments being offset by transform faults (see Figure 18-13). Earthquake epicenters coincide with the ridge crests and with the transform faults between the offset ridge segments, as shown in the figure. In 1967 seismologists at Columbia University found that the pattern of P-wave motions radiated from earthquakes on ridge crests indicated that they originate in normal faults that run parallel to the ridge crest. This means that the axis of tension is perpendicular to the trend of the fault, as we have seen in Figure 18-16. This finding is just as predicted by the plate-tectonics concept, which specifies that the ridge crests mark the boundary between separating plates. Furthermore, earthquakes in transform faults between ridge crests were found to show lateral slips, just as would be expected for a region where plates slide past each other in opposite directions. What elegant support seismology gives to the notion that plates spread from ridge crests! Outside the region between the ridge crests, the transform fault becomes **aseismic**—that is, it produces no earthquakes. This, too, is to be expected since in this region the plates move in the same direction on both sides of the fault. In a sense the fault has healed and is evidenced only by topography, usually by a scarp (cliff or steep slope), as shown in Figure 18-13.

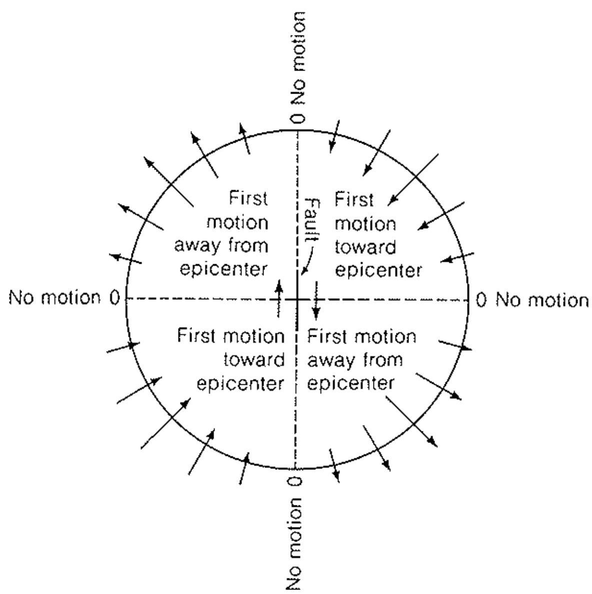

Figure 18-17

The initial motion of seismic waves shows a characteristic movement, a push away from the source or a pull toward it, depending on the orientation of the fault, the direction of slip along the fault, and the direction of the seismograph from the earthquake. The fault orientation and slip direction can be obtained from the dashed lines that separate the stations into quadrants of initial motion toward the epicenter or away from it. Because most earthquakes originate below the surface, seismologists must rely on this principle in analyzing their records to find the orientation of the fault and the direction of slip.

What about the leading edges on the other side of the moving plates, where collisions occur? Seismologists have found that many of the deep earthquakes that originate within the subducted plate show the predicted compressive mechanism in the direction of the dip of the downgoing plate (see Figure 18-13). They have also devised methods of mapping the downgoing plate by tracking the seismic waves, which are guided more efficiently up the cold plate from the earthquake focus to the surface than through the adjacent mantle, which is hot and muffles the waves. No earthquakes occur below 650 km. Presumably this is the depth of greatest penetration, of subducted plates, or the depth at which they "soften", or are resorbed in the mantle.

EARTHQUAKE DESTRUCTIVENESS— CAN IT BE CONTROLLED?

Earthquakes cause destruction in several ways. Ground vibrations can shake structures and stress them to the point of failure and collapse (Figure 18-18). The ground accelerations caused by great earthquakes can approach and even exceed that of gravity near the epicenter, and very few manmade structures can survive without severe damage. Certain kinds of soil lose their ridigity and "liquefy" when subjected to repeated seismic shocks. The ground simply slides away, taking buildings, bridges, and everything else with it (Figure 18-19). As was mentioned earlier, coastal earthquakes occasionally generate the awesome waves called tsunamis, which travel across the ocean at speeds of up to 800 km/hour (500 miles/hour) and form walls of water as much as 20 m high as they sweep over low-lying coastal areas (Figures 18-20 and 18-21). Avalanches, mudflows, and fire may accompany earthquakes and take their toll (Figure 18-22). Of the 99,000 fatalities in the Tokyo earthquake of 1923, 38,000 were due to fire. Table 18-2 lists the human losses of historical earthquakes. A seismic-risk map of the United States, based on the earthquake history of the country, is shown in Figure 18-23. You may be surprised to find that you live in a zone where there is risk of earthquake damage.

Can anything be done about reducing earthquake hazards? Seismologists in the United States, Japan, the Soviet Union, and China are working hard to find answers to this question. Even though no major scientific breakthroughs have been made so far, damage and loss of life can be mitigated by encouraging sound building practices. Figure 18-24 shows something that should not be allowed —a residential area built in an active fault zone, the San Andreas, the most dangerous in the United States. Construction on unstable soils or in avalanche-prone areas should be prohibited. Engineers can design structures that will withstand most earthquakes, and building codes should require that only such building be done in high-risk areas.

Twenty-five years ago only astrologers, mystics, and religious zealots were concerned with earthquake prediction. Today seismologists in many countries are actively working on this problem and can claim a few successes. In February 1975 an earthquake was predicted 5 hours before it occurred near Haicheng in northeast China. Several million people, prepared in advance by a public education campaign, evacuated their homes and factories in the hours before the shock. Although many towns and villages were totally destroyed, only a few hundreds lives were lost. Western scientists who have since visited the region estimate that tens of thousands of lives were saved. The Chinese have successfully predicted other earthquakes, but unfortunately they were able to provide only a long-term warning (within 5 years) of the great T'ang-shan earthquake of August 1976—not enough accuracy to save the 500,000 people estimated to have lost their lives. Smaller earthquakes have been predicted in the United States and the Soviet Union, in connection with the research programs in those countries.

The scientific basis of earthquake prediction is the subject of intensive research in the United States, Japan, China, the Soviet Union, and other

Figure 18-18
Destruction caused by the San Fernando, California, earthquake of 1971. [Photo by R. E. Wallace, U.S. Geological Survey.]

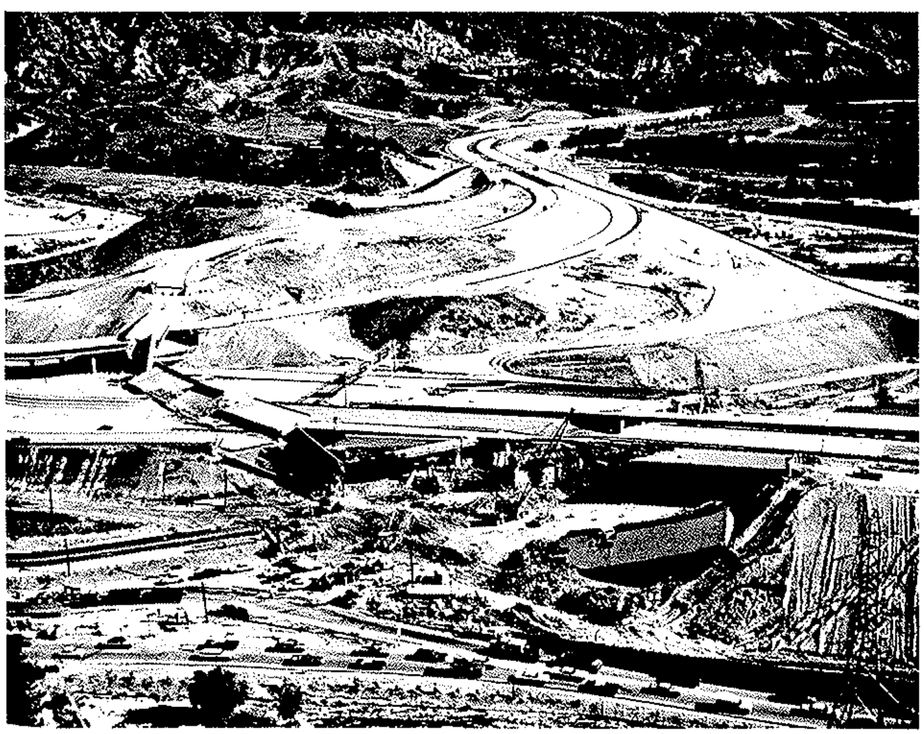

Figure 18-19

Foundation failure as a result of soil liquefaction caused these buildings in Niigata, Japan, to topple during the earthquake of 1964. The structures themselves were built to withstand earthquakes; they toppled intact. [Photo by G. Housner, California Institute of Technology; National Science Foundation.]

Figure 18-20

Destruction at Seward, Alaska, caused by the tsunami generated during the earthquake of 1964. Although a warning system exists to alert people on distant coasts to the danger of tsunamis, it cannot yet function rapidly enough to help residents in the epicenter region. [Photo by F. Press.]

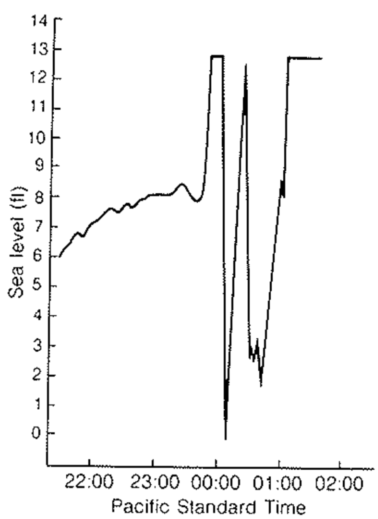

Figure 18-21

The tsunami from the great Alaskan earthquake of 1964 reached California, where several people perished and some coastal damage resulted from the waves. A tide gauge at Crescent City, California, which usually serves to record ocean tides, made this record of the tsunami, showing sea-level changes of almost 2 m more than normal.

Figure 18-22

Monument standing atop the debris of an avalanche that buried the town of Khait in the Tadzhik Republic of the Soviet Union following the earthquake of 1949; 12,000 people were killed. The slide, more than 30 m thick, moved over the town with a velocity of 10 m/s. No sprinter could have outrun it. [Photo by F. Press.]

Table 18-2

Some of the World's Worst Earthquakes as Regards Lives Lost

Year	Place	Deaths (est.)	Year	Place	Deaths (est.)
856	Corinth, Greece	45,000	1923	Tokyo, Japan	99,000
1038	Shansi, China	23,000	1930	Apennine Mountains, Italy	1,500
1057	Chihli, China	25,000	1932	Kansu, China	70,000
1170	Sicily	15,000	1935	Quetta, Baluchistan	60,000
1268	Silicia, Asia Minor	60,000	1939	Chile	30,000
1290	Chihli, China	100,000	1939	Erzincan, Turkey	40,000
1293	Kamakura, Japan	30,000	1948	Fukui, Japan	5000
1456	Naples, Italy	60,000	1949	Ecuador	6000
1531	Lisbon, Portugal	30,000	1949	Khait, U.S.S.R.	12,000
1556	Shen-shu, China	830,000	1950	Assam, India	1500
1667	Shemaka, Caucasia	80,000	1954	Northern Algeria	1500
1693	Catania, Italy	60,000	1956	Kabul, Afghanistan	2000
1693	Naples, Italy	93,000	1957	Northern Iran	2500
1731	Peking, China	100,000	1960	Southern Chile	5700
1737	Calcutta, India	300,000	1960	Agadir, Morocco	12,000
1755	Northern Persia	40,000	1962	Northwestern Iran	12,000
1755	Lisbon, Portugal	30,000–60,000	1963	Skopje, Yugoslavia	1000
1783	Calabria, Italy	50,000	1968	Dasht-e Bayaz, Iran	11,600
1797	Quito, Ecuador	41,000	1970	Peru	20,000
1822	Aleppo, Asia Minor	22,000	1972	Managua, Nicaragua	10,000
1828	Echigo (Honshu), Japan	30,000	1976	Guatemala	23,000
1847	Zenkoji, Japan	34,000	1976	T'ang-shan, China	500,000(?)
1868	Peru and Ecuador	25,000	1976	Philippines	3100
1875	Venezuela and Columbia	16,000	1976	New Guinea	9000
1896	Sanriku, Japan	27,000	1976	Iran	5000
1897	Assam, India	1500	1977	Rumania	1500
1898	Japan	22,000	1978	Iran	15,000
1906	Valparaiso, Chile	1500	1980	Algeria	3500
1906	San Francisco	500	1980	Italy	4000
1907	Kingston, Jamaica	1400	1981	Iran	3000
1908	Messina, Italy	160,000	1982	West Arabian Peninsula	2800
1915	Avezzano, Italy	30,000	1983	Turkey	1300
1920	Kansu, China	180,000			

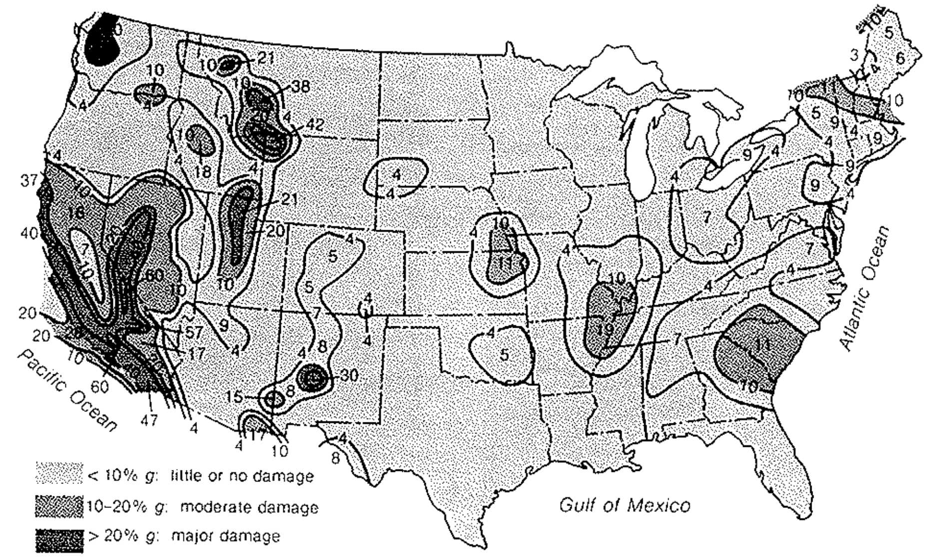

Figure 18-23

Expected level of earthquake-shaking hazards. The levels of ground shaking for different regions are shown by contour lines that express the maximum amount of shaking likely to occur at least once in a 50-year period as a percentage of the force of gravity. Damage begins to occur at about 10% *g*. An acceleration of 0.1% *g* or more is perceptible to people. [Modified from U.S. Geological Survey Chart.]

countries. Scientists are searching for premonitory indicators that would predict the time and place of a forthcoming destructive earthquake. Among the possible indicators being examined are unique, systematic patterns in the occurrence of smaller earthquakes in the general region prior to the impending main shock (Figure 18-25); the prior occurrence of surface deformation; unusual aseismic slip (creep) on faults; the occurrence along faults of strain changes that tend to reduce the friction between the two facing blocks, "unlocking" the fault; changes in physical properties of rock in the vicinity of faults; and unusual flow of underground water or release of trace gases.

Ask a seismologist to predict the time of the next great earthquake and the response is likely to be, "The longer the time since the last big one, the sooner the next great shock." This simplistic statement is the basis of the **seismic gap method,** which has successfully forecast the locations and magnitudes of more than six major earthquakes within a few years of their occurrence.

The seismic gap method has been most successful with earthquakes that occur on faults that mark plate boundaries. The basic idea is that earthquakes result from the accumulation along these faults of strain due to the steady motion of the plates. After buildup to some critical level of strain, the brittle lithosphere breaks. The cycle of slow strain accumulation and sudden release in an earthquake recurs over and over again with an average interval that varies from place to place. According to the method, the most likely place for an earthquake to occur is at a locked portion of a fault where an earthquake is "due," that is, where the time since the last earthquake has reached or exceeds the average interval between earthquakes for this location. The average recurrence interval can be estimated in a number of ways. The timing of great earthquakes going back several thousand years can be estimated by finding sedimentary layers that are offset by fault displacements and then dating these layers. In another method, the interval is given by the number of years of steady plate motion it takes to accumulate, or "store," the fault displacements that occurred in earlier earthquakes. (For example, it would take 150 years to accumulate a fault displacement of 6 m if the plate motion were 4 cm/year.) Although the different methods give similar results, the uncertainty of the prediction is unfortunately large—as much as 50% of the average recurrence time. This can amount to prediction with an uncertainty of many decades. However, the simultaneous use of the gap method and one or more of the premonitory indicators described earlier could sharpen the prediction.

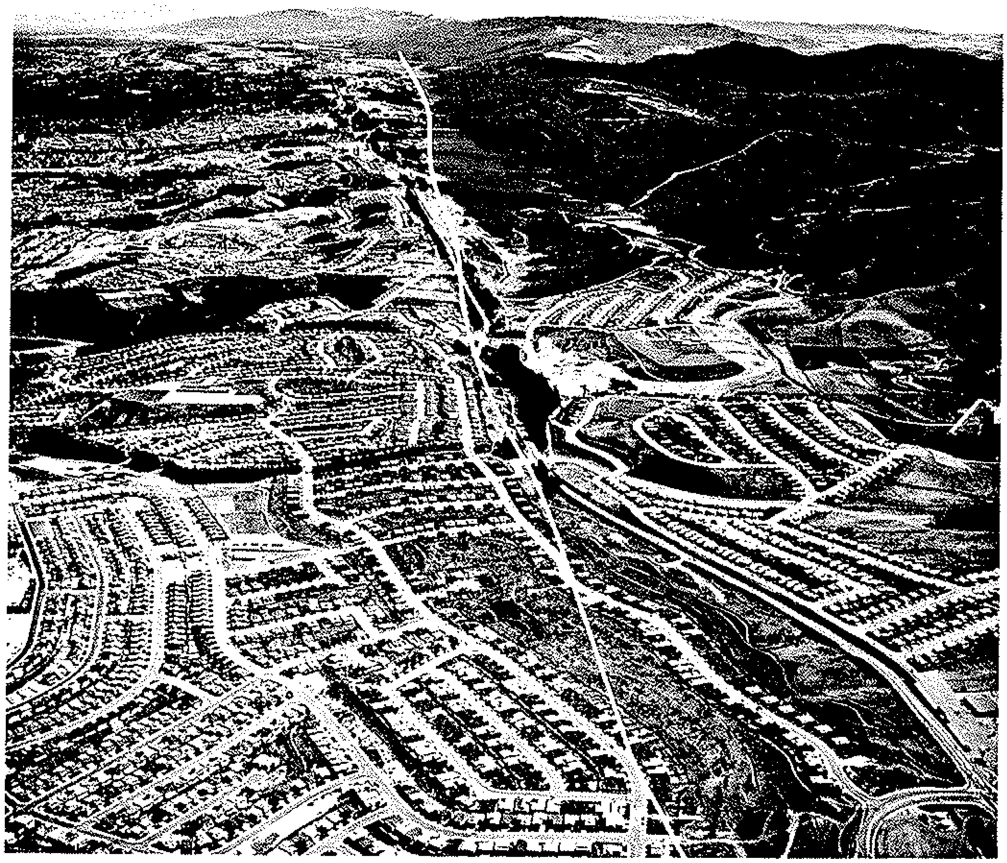

Figure 18-24

Housing tracts constructed within the San Andreas fault zone, San Francisco peninsula. The white line indicates the approximate fault trace, along which ground ruptured and slipped about 2 m during the earthquake of 1906. [Photo by R. E. Wallace, U.S. Geological Survey.]

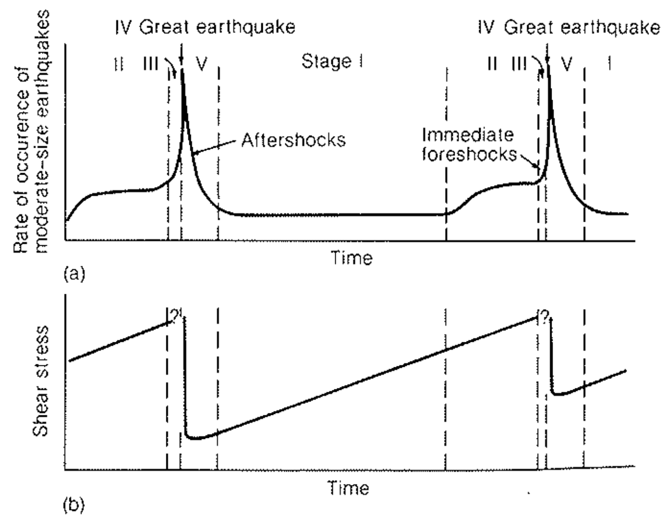

Figure 18-25

Model of cycle of repeating great earthquakes along a plate boundary such as the San Andreas fault. (a) Great earthquakes are followed by several years of declining aftershocks (stage V); most of the 50- to 500-year intervals between great earthquakes are characterized by low levels of seismic activity (stage I). Stage II, an increased level of earthquakes, occurs some decades before the main shock. Stage III may be measured in years, days, or hours before the main shock. Some seismologists believe that northern California is entering stage II, and that southern California may be entering stage III. (b) Movement of plates results in buildup of shear stress along the fault, which is released suddenly at the moment of a great earthquake (stage IV). [After C. B. Raleigh, K. Sieh, L. R. Sykes, and D. L. Anderson, *Science*, v. 217, pp. 1097–1104, 1982.]

The San Andreas fault of Southern California serves as a good example. The recurrence time between great earthquakes measured by the two methods is 100–150 years. The last great earthquake occurred in 1857; therefore an earthquake would be expected at any time—tomorrow or decades from now. However, since 1978 California has had a larger number of moderate-sized earthquakes than in the preceding 25 years. Southern California may have entered stage III, the last stage of seismic activity before a great earthquake (Figure 18-25). Geologists have also observed surface deformation of the kind that stretches the distance between points on opposite sides of the San Andreas, as if the fault were beginning to unlock. For these reasons seismologists now believe that a great earthquake is likely to happen in California in the next decade or so, with Southern California the most likely location. This is particularly worrisome because of the high density of population that now exists in the region. A 1980 government report estimates that if the 1857 earthquake were to recur, 10,000–15,000 deaths, 50,000 persons hospitalized, and $17 billion in property losses could be expected! These estimates could be too low or too high by a factor of 2 or 3. If the prediction could be improved so that a warning could be issued hours or days before the shock, the casualties could be reduced significantly.

Because of these concerns a major earthquake prediction and hazard mitigation program was initiated by the U.S. government in recent years. Similar activites are under way in other countries with high seismic risk.*

If earthquake prediction research has just become respectable, earthquake control continues to boggle the imagination. Yet some chance discoveries have opened this intriguing possibility. In 1966 a dramatic correlation was found between the rate of high-pressure injection of waste fluids into a deep well and the frequency of earthquakes in the vicinity of Denver, Colorado (Figure 18-26). Apparently the earthquakes were triggered by reduction of frictional resistance to faulting. The pressure exerted by the injected fluids "unlocked" a preexisting fault, and strains that had built up earlier were released. Perhaps someday earthquake-control wells will be spotted every few miles along the San Andreas fault, and fluid injected so as to cause the fault to creep continuously and slip frequently. These controlled earthquakes would prevent strain from building up over periods of 50–100 years and being released in a large, damaging shock. Much research will be needed to achieve this important (and perhaps impossible) goal; the first steps have already been taken.

*An ancient method of prediction used for centuries is based on unusual animal behavior in the few days or hours before an earthquake. Because of recent reports by trained observers in China and Italy, scientists no longer dismiss this "peasant wisdom" but are trying to check if, and why, it works.

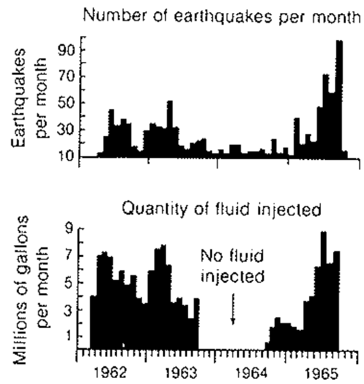

Figure 18-26

Correlation found by D. M. Evans between the quantity of wastewater injected into a deep well and the number of earthquakes per month in the vicinity of Denver, Colorado. This unplanned "experiment" opens the distant possibility of earthquake control by fluid injection.

Exploring the Interior with Seismic Waves

To appreciate the importance of seismic waves in revealing the properties of the interior, we need only reflect on what the state of knowledge would be in the absence of this key tool. We might surmise the existence of a crust from the observation that most surface rocks are light and felsic or mafic compared to the more dense ultramafic intrusions that seem to invade the surface layers from below, but we could only speculate on its thickness. The sea-floor crust would of course be terra incognita. We probably would have guessed the mantle to be composed of ultramafic rocks, but we could only wonder about its physical state, structure, and thickness. From the clues provided by iron meteorites, the large relative abundance of iron in the cosmos, and our efforts to explain the Earth's density and magnetic field, we might have been led to hypothesize the existence of a molten iron core, but this would have been argued extensively. Its depth would be uncertain, and the inner solid core would be unknown. Continental drift and sea-floor spreading would be debated, but the overall concept of plate tectonics—especially the fate of plates in subduction zones—would probably have escaped us.

TYPES OF SEISMIC WAVES

As early as the 1800s, mathematicians proved with pencil and paper the existence of compressional and shear waves in elastic bodies. Not until the close of the nineteenth century, however, did seismologists devise instruments sensitive enough to detect such waves in the Earth—the *P* waves and *S* waves generated by sudden slip along a fault. Figure 18-27 shows the faster-traveling *P* wave as the propagation of a volume change—a squeezing and unsqueezing of the medium; the individual particles vibrate to and fro in the direction of wave propagation. In Figure 18-28, the *S* wave is shown as a traveling shearing disturbance, the material

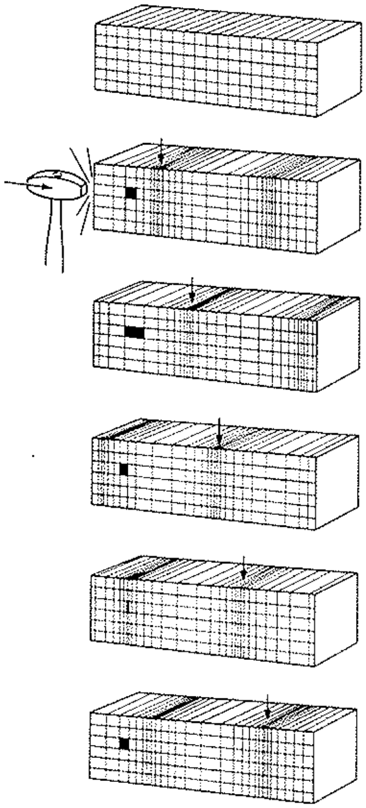

Figure 18-27

Stages in the deformation of a block of material with the passage of compressional *P* waves through it. The undeformed block is shown at the top. In the sequence from top to the bottom, a crest of compression, marked by an arrow, moves through the block with the *P*-wave velocity. It is followed by an expansion, and any small piece of matter, like the marked square, shakes back and forth in response to alternating compressions and expansions as the wave train moves through. A sudden push (or pull) in the direction of wave propagation, indicated by the hammer blow, would set up *P* waves. [After *The Heart of the Earth* by O. M. Phillips. Freeman, Cooper & Co. Copyright © 1968.]

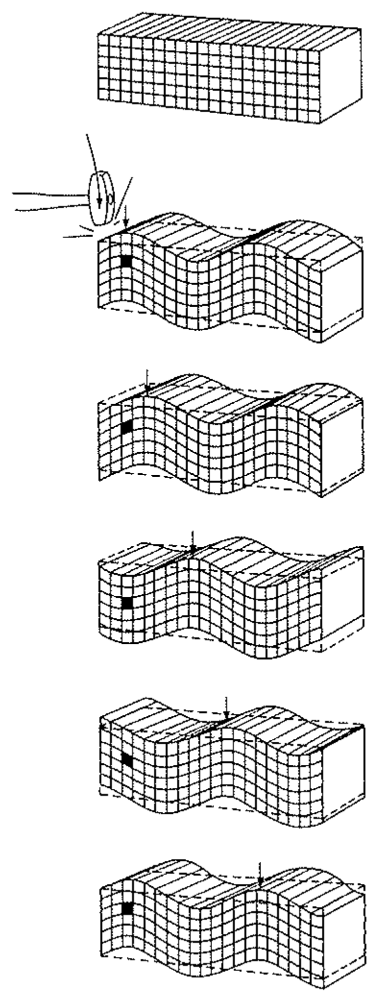

Figure 18-28

Stages in the deformation of a block of material with the passage of shear waves, or *S* waves, through it. A wave crest, marked by an arrow, moves through the block with the *S*-wave velocity as vertical planes shake up and down. Any small piece of matter, like the marked one, shakes up and down and experiences a shearing deformation (from a square to a parallelogram in the figure) as the shear wave passes through. A sudden shear displacement, indicated by the hammer blow at right angles to the direction of wave propagation, would set up *S* waves. [After *The Heart of the Earth* by O. M. Phillips. Freeman, Cooper & Co. Copyright © 1968.]

distorting in shape rather than changing in volume; the particles vibrate back and forth at right angles to the direction of propagation. *P* waves are a key tool for exploring sedimentary rock sections likely to contain oil or natural gas (Box 18-1).

Figure 18-29 depicts the paths of *P* waves as they travel from the source of an earthquake or explosion into the interior, emerging again at distant points. These wave paths and their travel times have been determined empirically from the seismographic records of earthquakes all over the world. The Earth's core deflects the waves and in effect casts a shadow where very little *P*-wave energy reaches the surface. The existence of such **shadow zones** suggested that the core is molten because compressional waves decrease sharply in velocity when they pass from a solid into a liquid of the same composition. The suggestion became a firm pronouncement when seismologists found that shear waves do not penetrate this region. Liquids transmit *P* waves but not *S* waves because the fluids elastically resist and recover from squeezing but do not resist shearing.

When *P* and *S* waves encounter a boundary like that between the core and the mantle, they are in general both reflected back and transmitted across it, just as light may be partly reflected and partly transmitted at a water surface. If in the new medium the wave velocity is different, the waves are bent, or **refracted.** Because of all of these possibilities of reflection, transmission, and refraction, *P* and *S* waves break up into several types as they travel through the Earth, as shown in Figure 18-30. Follow the wave *PcP* in the figure as it bounces—like a radar beam—from the Earth's core and yields the depth of the core from the round-trip time. The wave *PKP,* which penetrates the core, is useful for exploring that region. Many of the *P*-wave trajectories and travel times are sketched in Figure 18-29.

In addition to *P* and *S* waves, there is a third category of seismic wave, the surface wave, that travels along the Earth's surface. Surface waves are guided by the surface and the outer layers of the Earth, just as the motion of ocean waves is mostly surficial. Interestingly the chief difference seismologists found between earthquakes and underground nuclear explosions is in their ability to generate surface waves. Explosions excite surface waves with less efficiency than do earthquakes—a discovery that may stimulate statesmen to agree to an underground nuclear test-ban treaty. Figure 18-31 shows seismograms in which some seismic waves are labeled.

Pluck a violin string and a tone is emitted; strike

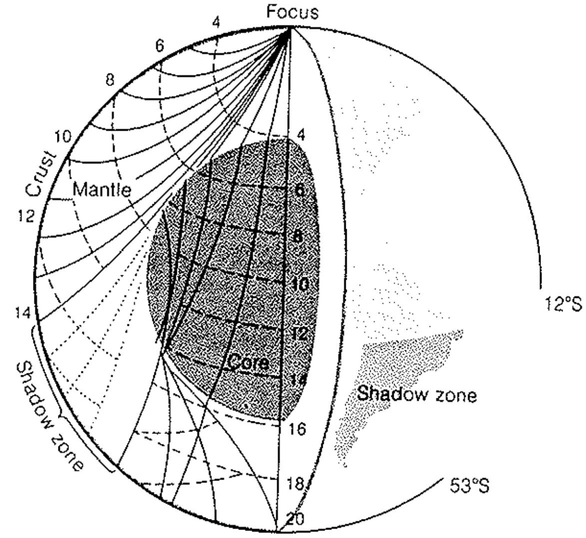

Figure 18-29

Cutout showing the pattern of *P*-wave paths through the Earth's interior. The numbers show the travel time in minutes for the waves to reach the associated broken line. Note the shadow zone, a region not reached by *P* waves (for this hypothetical earthquake at the North Pole) because they are deflected by the Earth's core. [After *Internal Constitution of the Earth* by B. Gutenberg, ed. Copyright © Dover Publications, 1951.]

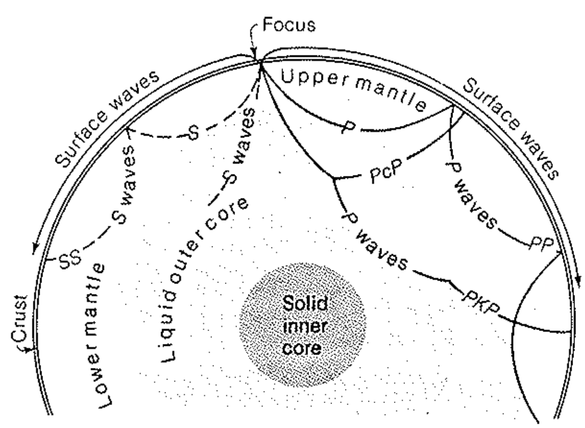

Figure 18-30

P and *S* waves radiate from an earthquake focus in many different directions. Waves reflected from the Earth's surface are called *PP* or *SS*. *PcP* is a wave that bounces off the core, and *PKP* is a *P* wave transmitted through the liquid core. *S* waves cannot travel in a liquid.

Box 18-1

Finding Oil with Seismic Waves

Exploration for oil is an important application of seismology. In offshore prospecting, a ship tows a sound source and underwater phones. *P* waves (sound waves) are generated by a pneumatic device that works like a balloon burst. The sound waves bounce off rock layers below the sea floor and are picked up by the phones. In this way subsurface sedimentary structures that trap oil, such as faults, folds, and domes, are "mapped" by the reflected waves. This technique is used extensively to explore the submerged continental shelves and shallow seas for oil and gas deposits. Oceanographers use this method to study the sedimentary layers on the continental slope and rise and on the floor of the deep sea.

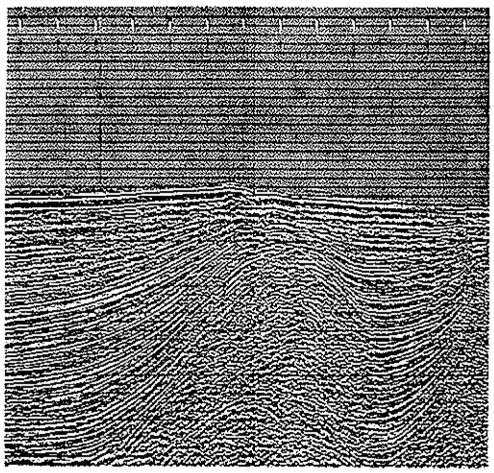

A section of the Gulf of Mexico, 30 km long and 10 km deep, in which folded sedimentary layers are revealed by reflected seismic waves. [From Petty Geophysical Engineering Co.]

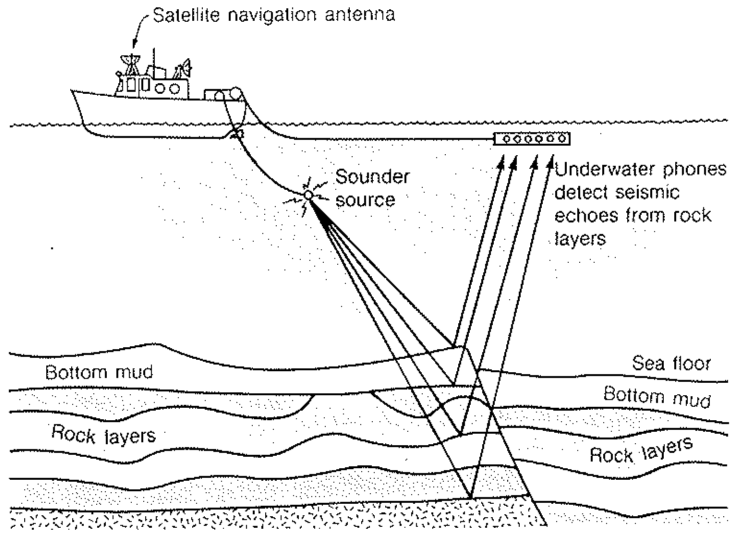

Seismic method of prospecting for oil and gas offshore. [After U.S. Department of the Interior.]

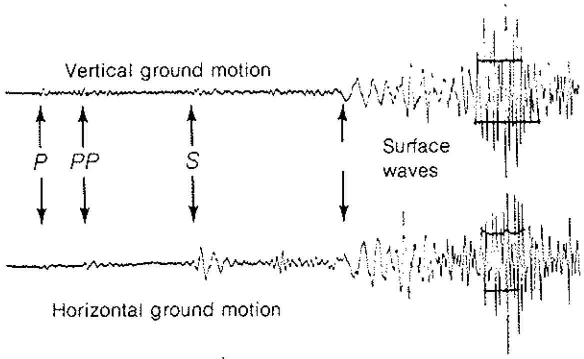

Figure 18-31

Seismograph recording of *P*, *S*, and surface waves from a distant earthquake.

a bell with a hammer and it rings. The Earth also rings when it is disturbed by a great earthquake that causes the entire globe to vibrate like a bell for as long as several weeks. The tones of Earth's vibrations are pitched too low for the human ear to hear, but modern seismographs are sensitive enough to detect these low-frequency oscillations. The Earth can vibrate in different ways, or modes, actually an infinite number of them. Some are shown in Figure 18-32. The mode with the lowest pitch is the "football," or *spheroidal,* mode, which takes 53 minutes to execute one vibration. For those of you who are musicians, this vibration corresponds to E flat in the twentieth octave below middle C. You might call this music of the spheres. The "balloon," or *radial,* mode has a frequency of one vibration in 20 minutes; and the twisting, or *torsional,* mode, a frequency of one in 44 minutes.

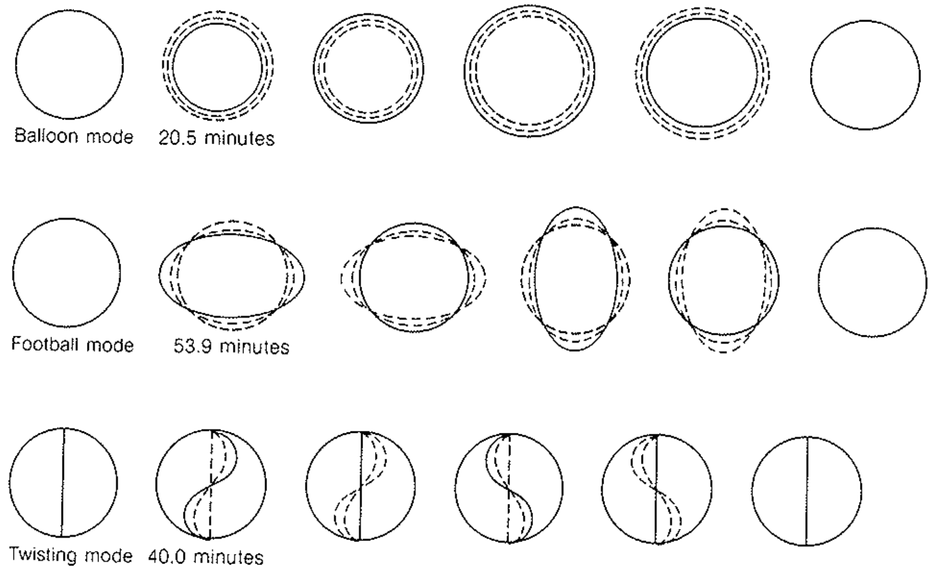

Figure 18-32

Three of Earth's vibrational modes. The schematic illustration shows how the planet changes shape and gives the time it takes to complete the sequence of vibrations shown. The actual movements are only a small fraction of a millimeter.

FINDING EARTH MODELS FROM TRAVEL TIMES AND VIBRATION FREQUENCIES

Using thousands of sensitive seismographs and highly accurate clocks, seismologists around the world measure precisely the travel times of *P, S,* and surface waves and the frequencies of the vibrations of the Earth. From these measurements they can plot travel-time curves of the kind shown in Figure 18-14 for the different kinds of seismic waves. The travel times depend on how the velocities of compressional and shear waves change as they pass through materials of different elastic properties. The vibration frequencies of the Earth depend on the velocities of these waves as well as on the density of different parts of the interior, just as the tone of a bell depends on its elasticity and density. Once all the seismological data are accumulated, the next step is to find Earth models whose *P*-wave and *S*-wave velocities and internal densities are consistent with the data.

Solving this "inverse problem," as it is called by mathematicians, is something like being told that a driver made a trip from Los Angeles to San Francisco in 7 hours, in bad weather, on a Monday, and having to make a best guess of the route he took. The mathematics of this process cannot be explained here, but the techniques are powerful enough to allow us to make a best estimate of an Earth model.

A plot of internal densities and *P*- and *S*-wave velocities for the Earth is given in Figure 18-33. It is quite likely that these curves represent the real Earth within a percent or so. As more complete and more precise data become available, these curves should become more accurate, perhaps someday converging to give us a perfect model of the real Earth. But what can we say *now* about the interior?

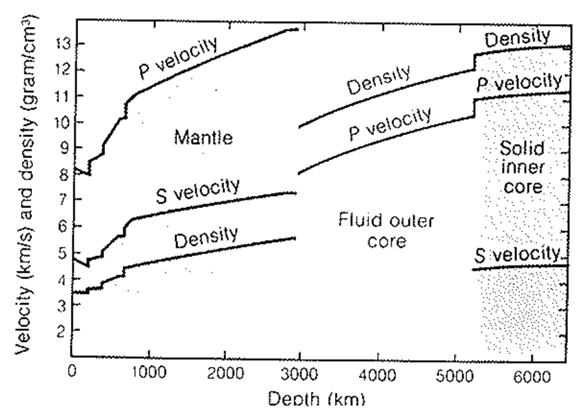

Figure 18-33

Estimate of the variation in density and in *P*- and *S*-wave velocities in the Earth's mantle and core. Uncertainty is probably only a few percent of the actual value. [Prepared by A. M. Dziewonski and D. L. Anderson for the Standard Earth Committee of the International Union of Geodesy and Geophysics.]

COMPOSITION, STRUCTURE, AND STATE OF THE INTERIOR

Velocity and density models are important mainly as a means to an end; the ultimate goal is to understand the composition, structure, and state of the Earth's interior. Laboratory experiments make the connection between seismology on one hand and petrology and geochemistry on the other. High-pressure equipment and shock waves generated by explosives are used, as described in Box 18-2, to learn how velocity and density would vary in different rocks, either in the solid or in a partially molten state, and either near the surface or in the deep interior. With this information the Earth model shown in Figure 18-33 can be interpreted to give information about the materials and their state.

The major divisions, crust, mantle, and core (see Figure 18-30), were discovered from the analysis of reflected and refracted *P* and *S* waves and have been known for more than 60 years. The boundary between the crust and the mantle is called the **Mohorovičić discontinuity** (**M,** or **Moho,** for short) after the Yugoslavian seismologist who discovered it in 1909. It separates rocks in which *P* waves have velocities of about 6–7 km/s (3.8–4.4 miles/s) from underlying mantle rocks, in which *P* waves have a velocity of about 8 km/s (5 miles/s). The field method of measuring these velocities is described in Box 18-3. From geological sampling to find all possible crustal and mantle materials and from laboratory measurements of the properties of these materials, we have learned to associate *P*-wave velocities with composition, as indicated in Table

Box 18-2

High Pressure and Shock Experiments

Even if we knew in detail how density and seismic velocities change with depth in the Earth, we would still want to identify the materials and describe their physical conditions. To do this we also need information on the densities of different materials and the velocities with which seismic waves travel through them under the high pressures and temperatures that exist in the interior of a planet. The pressure at the center of the Earth is nearly 4,000,000 times atmospheric pressure,* and temperatures there range to several thousand degrees. Using a hydraulic press, geophysicists can squeeze rocks in the laboratory to pressures of about 100 kilobars, heat them to temperatures of about 1000°C, and at the same time measure many of their properties. This procedure duplicates conditions at depths of about 300 km. A recent technical breakthrough now makes it possible to increase laboratory pressures to 1.7 megabars and temperatures to 3000°C, conditions similar to those in the Earth's core. The experiment is similar to that depicted in the figure except that a diamond anvil is used. The sample is squeezed between two cut diamonds and heated by a laser beam.

Another technique for compressing rocks to very high pressures happens to be the very same method used to compress uranium when triggering an atomic explosion. An ordinary chemical explosive, such as dynamite, is wrapped around the rock. When the dynamite is detonated, the shock wave squeezes the rock, raising the pressure and temperatures to the high values needed to duplicate conditions at great depths. The rock is destroyed in the process, but in the few millionths of a second before it falls apart, data needed to calculate the density, pressure, and shock velocity (which is simply related to the seismic-wave velocities) are obtained electronically from sensors on the rock.

Other types of experiments are used to determine such things as strength and thermal, electrical, and elastic properties at high pressures and temperatures.

*Pressure is measured in atmospheres (atm), bars, or pounds per square inch (p.s.i.). 1 atm = 1.01 bars = 14.7 p.s.i. Geologists tend to use bars, kilobars (10^3 bars), and megabars (10^6 bars).

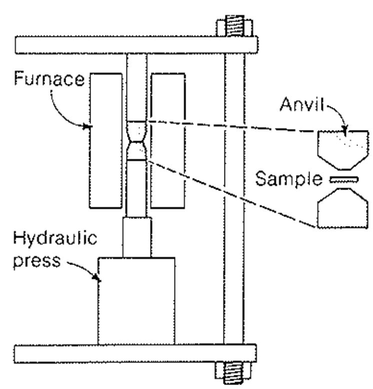

The Bridgman "squeezer," a device for subjecting minerals to pressures of a few tens of thousands of atmospheres and temperatures of several hundred degrees. The low pressure of the hydraulic press is amplified by concentrating the total force on the small area of the anvil. A furnace surrounding the anvil supplies heat. This apparatus simulates environments deep in the Earth's crust.

Box 18-3

Seismological Sounding of the Earth's Crust and Upper Mantle

Seismologists have developed a field procedure for measuring the thickness of the crust and the velocity of P waves in the crust and at the top of the mantle. Small seismometers are placed on the surface in a line extending away from a "shot point," where an explosion is set off to generate P waves. The waves leave the explosion in all directions—some traveling along the surface, others along the top of the mantle, as shown in the upper figure. A travel-time curve can be plotted on which each point represents the travel time required for the waves to reach a seismometer. The plot of waves that travel along the surface is a straight line through the origin of the graph with a slope of $1/V_1$. The slope of the line is measured to obtain the speed, V_1, of P waves in the crust. The waves traversing the mantle give a line with slope $1/V_2$ and intercept T. Values of V_1, V_2, and T obtained from the graph are used to calculate the thickness from the formula

$$D = \frac{T}{2} \frac{V_2 V_1}{\sqrt{V_2^2 - V_1^2}}$$

If you are familiar with trigonometry and Snell's law, you might try deriving this simple but important equation.

The lower figure shows seismic waves recorded at a distance of 163 km from an explosion of TNT. The traces are recorded from six seismometers placed 100 m apart. The waves that have traveled through the crust and mantle are denoted by P_1 and P_2, respectively.

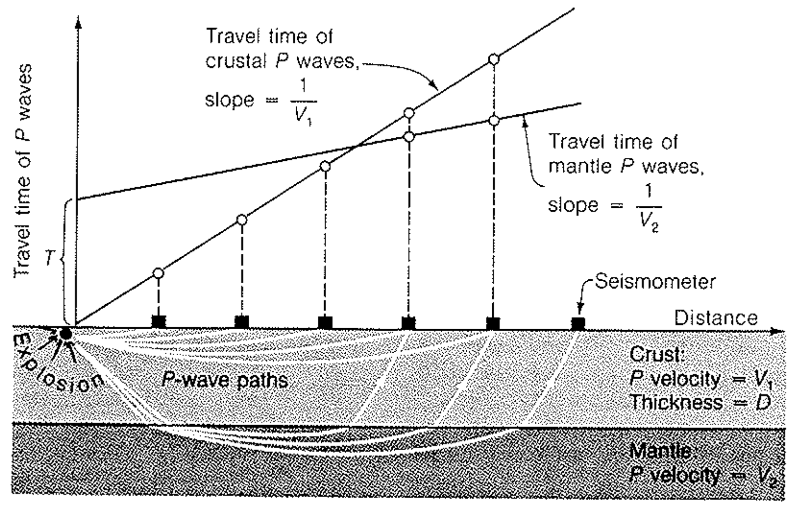

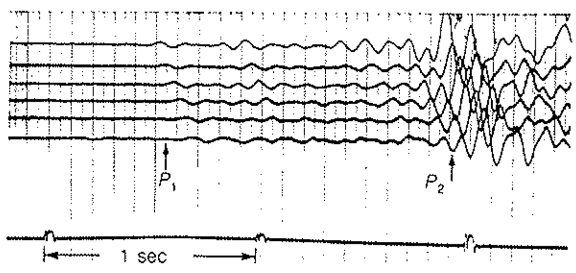

18-3. We conclude from these measurements that the continental crust consists mostly of granitic rocks, with gabbro appearing near the bottom, and that no granite occurs on the floor of the deep ocean, the crust there being entirely basalt and gabbro. The mantle below the M discontinuity is almost certain to be primarily the dense ultramafic rock peridotite. The crust is a distillate of the mantle and therefore differs chemically from its parent. In this sense, the Moho is a chemical boundary located by seismic waves.

Nowadays seismologists are excited by the finer details, the variation within the crust, mantle, and core. The variation in crustal thickness in a section

Table 18-3

Correspondence between Composition and *P*-wave Velocity in Igneous Rocks

Composition	*P*-wave velocity (km/s)
Felsic (granitic)	6
Mafic (gabbro)	7
Ultramafic (peridotite)	8

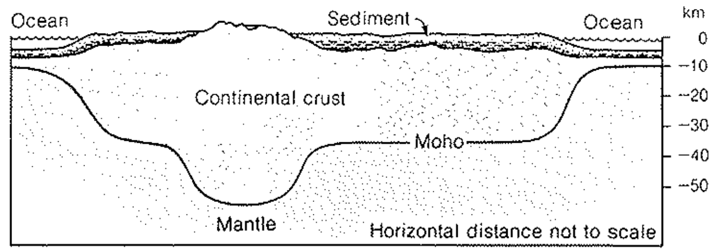

Figure 18-34
The lithosphere is topped by a relatively lightweight crust. Seismology reveals that the crust varies in thickness; it is thin under oceans, thicker under continents, and thickest under high mountains.

like the one shown in Figure 18-34 is one of the most important recent seismological results. The thickness of the crust varies from about 35 km to 10 km in a section extending from continent to ocean. Under a high mountain the crust thickens to as much as 65 km. If Figure 18-34 suggests to you that the continental crust floats on the denser mantle like an iceberg on the ocean, you have made a good observation. Icebergs float because they are less dense than seawater; flotation comes from the large volume of ice below the sea surface. When Archimedes' principle of buoyancy is applied to the flotation of continents and mountains, it becomes the **principle of isostasy,** which holds that the relatively light continents float on a more dense mantle; most of a continent's volume lies below sea level for the same reason that most of an iceberg lies below the ocean surface. Nature has contrived that large topographic loads such as mountains and continents are *compensated*—that is, supported primarily by buoyancy rather than by the strength of the crust. Rocks, which we know to be solid and strong over the short term (seconds or years), are, over the long term (thousands to millions of years), weak and flow like a viscous fluid when loaded. When continents grow or mountains are pushed up, a supporting root must develop as part of the process to provide buoyancy and keep the new load from sinking.

There is one variant to this general mechanism. If for some reason—for example, regional heating —part of the upper mantle becomes less dense than the adjacent mantle, it will also exert a buoyant force that can support elevated topography above it without the need for a crustal root. In a sense, the lower-density mantle serves as a root. This mode of isostatic compensation seems to be operating in the Basin and Range province (Utah, Arizona, Nevada) of the United States. The high heat flow in this region is consistent with the explanation. Seismological studies of crustal thickness have provided quantitative corroboration for the mechanism of isostasy.

In the years 1965–1970, geologists and geophysicists the world over concentrated research efforts on the upper thousand kilometers of the Earth as part of the International Upper Mantle project. This concerted attack led to many exciting discoveries about a region that had previously been poorly known. We can illustrate the more important of these by discussing the shear-wave velocity model. According to this model the mantle is divided on the basis of shifts in velocity into zones a–g (Figure 18-35). Zone a is the **lithosphere,** a slab up to about 70 km (45 miles) thick in which the continents are embedded. Crust forms the uppermost part of this outer shell of the Earth. Its lower boundary is marked by a decrease in shear-wave velocity. The lithosphere is characterized by high velocity and efficient propagation of seismic waves, both of which imply solidity and strength.

Zone b is the **asthenosphere,** or zone of weakness. It is also called the **low-velocity zone** for the obvious reason that the shear-wave velocity there is reduced. Seismic waves are attenuated more strongly in the asthenosphere than anywhere else in the Earth. Because laboratory experiments show that seismic waves are slowed and absorbed in a crystal–liquid mixture, some geophysicists think that the asthenosphere contains a small quantity of melt. Others believe that the low velocity is due to chemical or other physical changes. We have already noted that the Earth's lithosphere is made up of about ten distinct plates, created along mid-ocean ridges and destroyed in subduction zones. A solid slab underlain by a weak layer

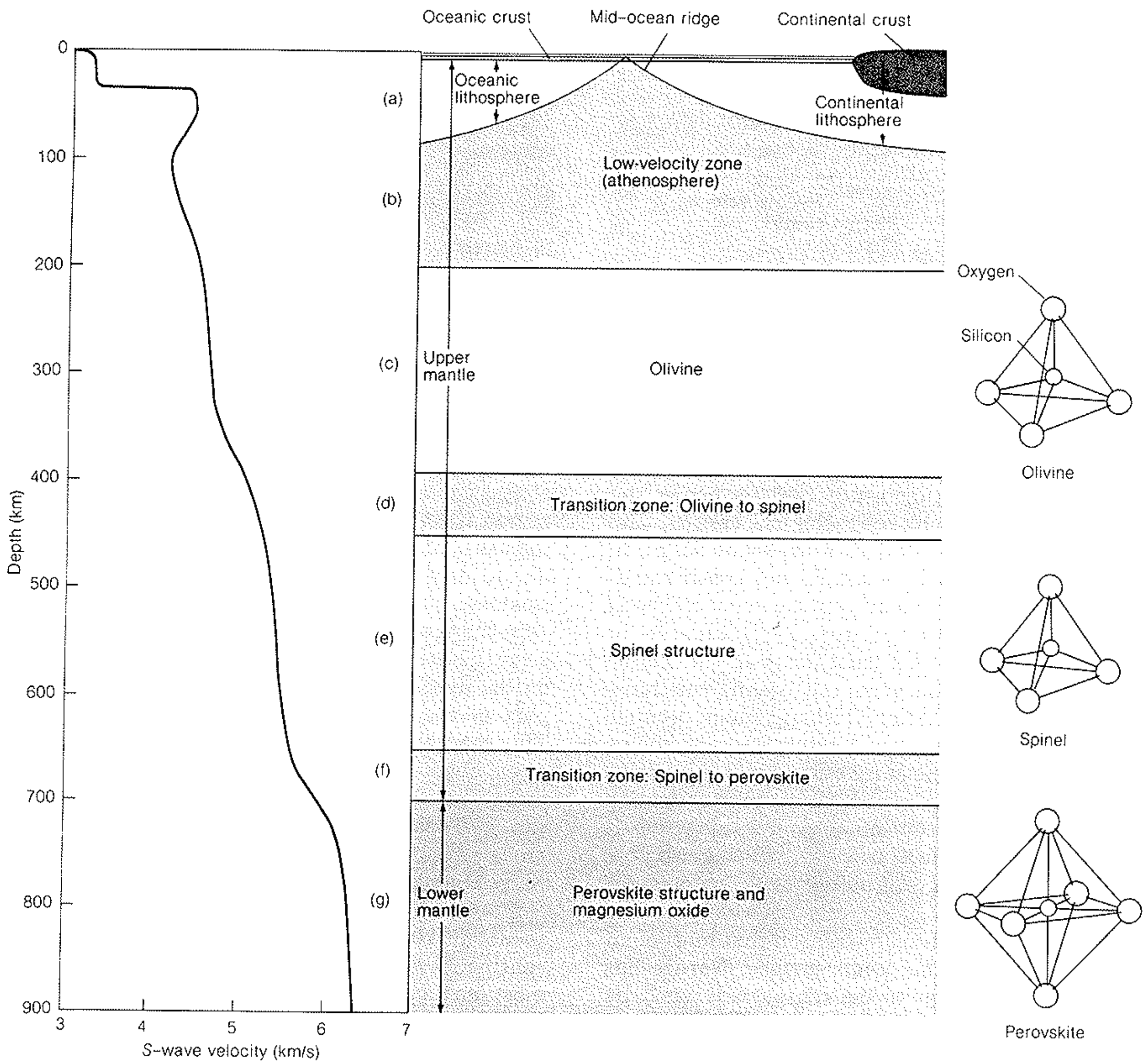

Figure 18-35

A modern view of the structure of the upper mantle, the outermost 700 km of the Earth, is illustrated by a plot of *S*-wave velocity against depth. Note how changes in velocity mark the strong lithosphere (a), the weak low-velocity zone (asthenosphere) (b), and the two transition zones (d and f). The transitions occur because increasing pressure forces a rearrangement of the atoms into more dense crystalline structures, from olivine to the spinel structure in zone d and from spinel to the perovskite and magnesium oxide (not shown) structures in zone f. The lower mantle may also differ chemically from the upper mantle. [After "The Earth's Mantle" by D. P. McKenzie. Copyright © 1983 by Scientific American, Inc. All rights reserved.]

might be more easily movable, and perhaps this accounts for the mobility of the lithospheric plates.

Velocity and density in both the lithosphere and asthenosphere fit a peridotitic composition. These two zones, therefore, do not differ so much chemically as they do in physical properties. In Chapter 16 it was proposed that the melt of the asthenosphere is the primary source of basaltic magma, which fits the picture nicely.

The asthenosphere ends at a depth of about 200 km (125 miles), and the rocks become solid again in zone c. The velocity increases gradually with depth in this region because of the effect of increasing pressure.

Zone d, about 400 km (250 miles) below the surface, is thin but very important. The rapid increase in velocity there correlates with the rapid increase in density in Figure 18-33. This transition is too abrupt to be accounted for by a chemical (composition) change. A physical change of phase—that is, a closer repacking on the atomic level—is required. The theoretical explanation was beautifully verified in 1969 when E. A. Ringwood and S. Akimoto squeezed olivine in their laboratories and found that at critical pressures and temperatures its atoms take up a more compact arrangement, changing into the spinel structure (Figure 18-35). Olivine is the principal mineral in peridotite, and at a depth of about 400 km in the Earth conditions are just right for it to change phase. This is an excellent example of how the collaboration of specialists with different backgrounds (seismologists and petrologists) can, little by little, remove some of the mystery of Earth's interior.

Zone e is one of gradual change with depth. However, zone f, near 670 km, shows a rapid change that seems to require both a physical change and a chemical change between the upper mantle above and the lower mantle below. Laboratory measurements show that phase changes involving a breakdown to denser molecular structures should occur at this depth.

The lower mantle, zone g, extending from 700 km (435 miles) to the core at a depth of 2898 km (1800 miles), is a region that changes little in composition and phase with depth. Density and velocity increase gradually, again due to increasing pressure.

The Earth's core is far away but not out of the reach of seismic waves. We know that its outer region is fluid and its inner one solid (see Figure 18-30). To obtain its composition, we use the same approach that has already proved so useful—comparison of laboratory experiments and seismological data. Look at Figure 18-36 to see how this is done. The density in the fluid core is plotted. Also shown are the densities of nickel, iron, and a mixture of iron and silicon, determined by "shocking" these materials in the laboratory with explosives, as was described in Box 18-2. We see that nickel is too dense. Iron is better but needs to be lightened by adding perhaps 15% silicon. Would other elements fit the data? Perhaps, but our choice is limited by the relative abundance of elements. Because the core accounts for one-third of the mass of the Earth, it must contain relatively abundant elements. Iron is the only abundant element that approaches the required density under the pressure of millions of atmospheres at these great depths. It is a little too dense, as Figure 18-36 shows, so a plentiful "lightening" element like silicon must be added. Oxygen or sulfur might also be a possible lightening element.

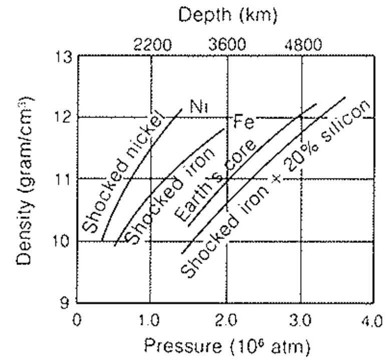

Figure 18-36

Density in the Earth's fluid core plotted against depth below the surface and against pressure (black curve). Comparisons with the densities for iron, nickel, and iron–silicon mixtures measured in laboratory studies enables seismologists to conclude that the core is mostly iron but slightly less dense than pure iron, as if a small amount of a "lightening" element like silicon were present.

In this way seismological observations and laboratory measurements of the properties of materials combine to give an incomplete but nevertheless good approximation of the Earth's interior. A zoned, differentiated Earth is found in which the major components are a metallic iron core and a rocky mantle consisting primarily of iron–magnesium silicates. The mantle includes a transition zone in which atoms are forced into closer packing, a partially molten asthenosphere, and most of the outer lithosphere. A thin, lightweight crust—the end-product of the differentiation process—caps the mantle.

The future holds even greater promise in exploring the Earth's interior. **Computerized tomography** (CAT–scanners) is a powerful tool used in medicine to reconstruct images of organs by using a computer's ability to calculate small differences in x rays that sweep the organ in many different directions. Seismologists have adapted the method, using seismic waves that sweep the mantle, and are constructing images of pieces of subducted slabs, the rising plumes of hot spots, and other discrete structures. The method may also detect convection in the mantle by picking up small changes in the speed of seismic waves due to a systematic orientation of mineral grains in the direction of convective flow. As in all fields of science, new tools will lead to new understanding in the continuing quest to understand our planet.

Summary

1 Most earthquakes originate in the vicinity of plate boundaries. The mechanism of earthquakes is governed by the kind of plate boundary: Fracture under tensile stress occurs at boundaries of divergence, fracture under compressive stress at boundaries of convergence, and lateral slip along transform faults.

2 Great earthquakes release in a few minutes huge amounts of elastic strain energy that had been slowly stored in the rocks of the fault zone over tens or hundreds of years. The source of this strain is plate motions.

3 Richter magnitudes are determined from the size of the ground motions, as measured when seismic waves are recorded on seismographs. The three types of seismic waves are P waves, S waves, and surface waves. The entire Earth can be set into global vibration by great earthquakes.

4 From a study of the travel times of seismic waves and the frequency, or pitch, of the global oscillations, seismologists have found that the Earth is divided into shells—that is, it is a zoned, differentiated planet, with

- a strong, slablike, mostly ultramafic lithosphere, broken into large, mobile plates;
- a weak asthenosphere, the primary source of basaltic magma, characterized by reduced velocity and high absorption of seismic waves;
- transition zones, where atoms are forced into a closer packing by the high pressures;
- a lower mantle, mainly iron–magnesium silicate;
- a fluid outer core, mostly iron but with one or more "lightening" elements; and
- a solid iron central core.

5 The continents with their lightweight felsic crusts—the end products of the differentiation process—are embedded in the lithosphere.

Exercises

1 What is an earthquake? How is its magnitude measured? How many earthquakes cause serious damage each year?

2 How does the distribution of earthquake foci correlate with the three types of plate boundaries?

3 Destructive earthquakes occasionally occur within plates, removed from plate boundaries. Why?

4 Seismograph stations report the following $S-P$ time differences for an earthquake: Dallas, $S-P$ = 3 minutes; Los Angeles, $S-P$ = 2 minutes; San Francisco, $S-P$ = 2 minutes. Use a map of the United States and travel-time curves (see Figure 18-14) to obtain a rough epicenter.

5 Taking into account the possibility of false alarms, reduction of casualties, mass hysteria, economic depression, and other possible consequences following an earthquake prediction, do you think the objective of predicting earthquakes is a worthwhile goal?

6 At a place along a boundary fault between the Nazca plate and the South American plate, the relative plate motions are 11.1 cm/year. The last great earthquake, in 1880, showed a fault slip of 12 m. When should local residents begin worrying about another great earthquake?

7 You wish to determine the depth to the water table before drilling a well. Using small explosions and seismographs you find that the P-wave velocity in the surface sediment is 600 m/s and the velocity in a subsurface layer, presumably the water table, is 1500 m/s. The intercept time, T, is 0.8 s. How deep is the water table? (See Box 18-3.)

8 Draw a cross section of the Earth, showing to scale the crust, lithosphere, asthenosphere, transition zone, core–mantle boundary, fluid outer core, solid inner core. What are the major characteristics of each region?

Bibliography

Anderson, D. L., "The San Andreas Fault," *Scientific American,* November 1971.

Board of Earth Sciences, National Academy of Sciences, *The Lithosphere.* Washington, D.C.: National Academy Press, 1983.

Bolt, B. A., "The Fine Structure of the Earth's Interior," *Scientific American,* March 1973.

Isacks, B., J. Oliver, and L. R. Sykes, "Seismology and the New Global Tectonics," *Journal of Geophysical Research,* v. 73, pp. 5855–5899, 1968.

McKenzie, D. P., "The Earth's Mantle," *Scientific American,* September 1983.

Office of Earth Sciences, National Research Council, *Trends and Opportunities in Seismology.* Washington, D.C.: National Academy of Sciences, 1976.